Lancaster University

How does dysregulation of DNA sensing cause the autoinflammatory syndrome SAVI?

Joshua Kimble

This dissertation is submitted for the degree of Msc (by research) Biomedical Science

Department of Biomedical and Life Sciences

November 2022

I declare that this thesis is my own work and has not been submitted in part, or as whole, for the award of a higher degree elsewhere

Table of Contents

List of Figures

List of Tables

Acknowledgements

Firstly, I would like to thank my supervisor Dr Leonie Unterholzner for her valuable input and support throughout this project. I would also like to thank all of the members of the Unterholzner lab for helping me throughout my time in the lab.

Abstract

STING was initially thought to be an adaptor protein with its sole role dependent on pattern recognition receptor (PRR) detection of cytosolic double stranded DNA leading to IRF3 driven canonical pathway activation. However, more recent research demonstrates STING as a signalling hub also capable of activation downstream of DNA damage. DNA damage induces a proinflammatory noncanonical STING response primarily through NF-κB. NF-κB promotes DNA damage repair or cell senescence and clearing however, is associated with autoinflammatory diseases when unregulated. STING-associated vasculopathy with onset in infancy (SAVI) is a rare yet severe autoinflammatory disease initially thought to be caused by hyperactivation of the canonical STING pathway, but knockout of signalling components in mice with the disease did not change its severity or outcome. To investigate the signalling cascades responsible for hyperactivation of the innate immune system, STING-deficient human HaCaT keratinocytes have been reconstituted with the SAVI inducing STING V155M mutant. Analysis of these SAVI-STING cells revealed constitutive hyperactivation of proinflammatory cytokines such as CCL2, CCL20, and IL-6 that are primarily associated with the non-canonical STING pathway, and further activation upon etoposide-induced DNA damage. H-151 induced STING inhibition downregulated proinflammatory cytokine expression, confirming the STING V155M mutant was responsible for the proinflammatory signalling profile, providing insight into the pathophysiology of SAVI patients.

1 Literature Review

1.1 Overview of the innate immune system

The innate immune system provides rapid and non-specific detection of pathogens from birth. This is achieved by germline-encoded pattern recognition receptors (PRRs) found on both immune and non-immune cells, which bind to conserved molecular motifs known as pathogen-associated molecular patterns (PAMPs) (Janeway and Medzhitov, 2002). As seen in ***Figure 1***, PRRs are located both on the cell membrane or in endosomes to detect and react to PAMPs from pathogens like viruses during all lifecycle stages. The rapid response that follows usually allows the innate immune system to locally eliminate pathogens. However, if unable to contain an infection, innate antigen presenting cells (APCs) such as dendritic cells (DCs) and macrophages interact and present antigens via major histocompatibility complex class I (MHC-I) and class II (MHC-II) molecules to T-cells to initiate the adaptive immune responses (Blum et al., 2013). Antigen receptors of T and B lymphocytes of the adaptive immune system provide long-term memory of individual pathogens, allowing a specific and fast response upon secondary infection (Cooper and Alder, 2006). Activation of the adaptive immune system also suppresses the innate immune system to prevent overactivation and collateral damage (Kim et al., 2007).

The innate immune system also has a vital role in cell homeostasis. First introduced as the danger model based on alloimmunity mediated allograft rejection, and the self and non-self-discrimination theory of immune responses, PRRs can also be activated by ligands that are not associated with pathogens (Land et al., 1994, Matzinger, 1994). Instead, these are host derived molecules released by damaged or dying cells known as damage-associated molecular patterns (DAMPs). Potential DAMPs can function normally within cells, however, can lead to sterile inflammation upon cellular stress. For example, cell damage induced oxidative stress and necrosis can release HMGB1 and DNA due to cellular membrane damage (Scaffidi et al., 2002). This change in localisation allows HMGB1 and DNA to function as a DAMP that binds to PRRs outside of the nucleus, leading to NF-κB and inflammasome pathway activation (Klune et al., 2008). Although inflammation can lead to tissue repair and regeneration, DAMPs

can induce unregulated inflammation and subsequent chronic autoinflammatory conditions, tissue destruction, and inflammation-driven tumour progression.

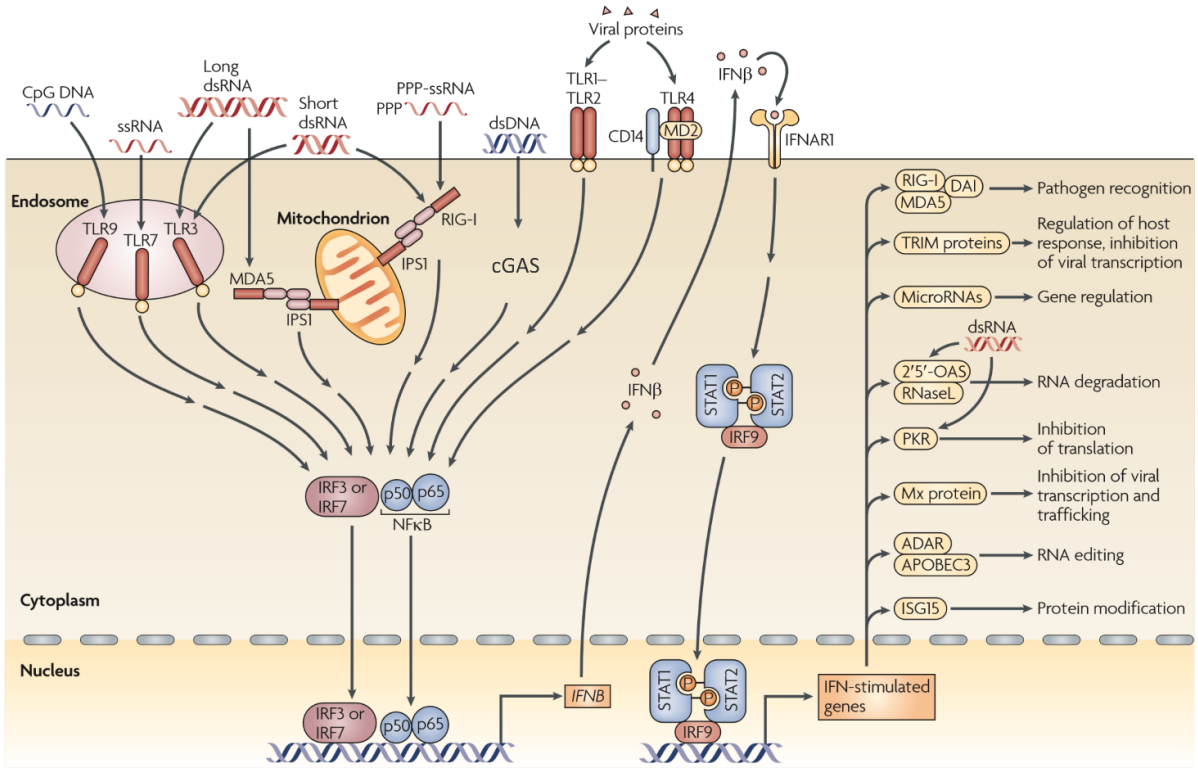

Figure 1. Overview of viral PAMP detection by PRRs.

Detection of viral PAMPs induces nuclear import of transcription factors IRF3/7 and NF-κB which promotes expression of type-I interferons and pro-inflammatory cytokines, respectively. Subsequent autocrine and paracrine signalling induces anti-viral innate immune responses including increased PRR expression, RNA degradation, and inhibition of cellular components needed for the viral lifecycle. Figure modified from Bowie and Unterholzner, (2008).

1.1.1 Anatomical and physical barriers

Anatomical and physical barriers are the first defences of the innate immune system, and include mucociliary clearance for airway surfaces, low stomach pH, antimicrobial activity of lysozyme within mucosal secretions, and primarily the skin (Bustamante-Marin and Ostrowski, 2017, Ferraboschi et al., 2021).

The skin is responsible for retention of fluids, temperature homeostasis, and protection against UV, which is achieved through constant replenishment of keratinocytes from the basal epidermis to form the epidermis (Lim et al., 2013).

The epidermis is structurally robust due to histidine-rich keratohyalin granules within the granular layer that bind cells together via keratin intermediate filaments (Sandilands et al., 2009). The stratum corneum on the surface of the epidermis consists of multiple layers of dehydrated keratinocytes that are constantly shedding to prevent infection (Rawlings and Matts, 2005). Secreted antimicrobial peptides (AMPs) from keratinocytes, fibroblasts, sweat glands, and skin resident innate immune cells are an element of humoral innate immunity and is the most effective form of active protection on the skin, consisting of two groups (Niyonsaba et al., 2017). The skin is under constantly exposure to the environment and pathogens, therefore, employs physical barriers, biochemical, and skin resident immune cell strategies that act in coordination and prime adaptive immunity if necessary.

1.1.2 Humoral innate immunity

Humoral innate immunity is one of the broadest components of the innate immune system as it consists of multiple families of soluble proteins found throughout the body. Humoral innate immunity consists of AMPs, natural antibodies (NAb), complement proteins, and pentraxins.

1.1.2.1 Antimicrobial peptides

As mentioned previously AMPs are one of the most effective elements of the innate immune system found on the skin. AMPs are also found in other areas of the body including hbD-5 and hbD-6 expression by epididymis (Yamaguchi et al., 2002). Although cathelicidin LL-37 is produced by keratinocytes, it is primarily expressed by neutrophils, macrophages, and mast cells which can be found circulating throughout the body (Alalwani et al., 2010, Niyonsaba et al., 2001). LL37 aids innate immune cells in both pro-inflammatory and antipathogenic roles, as well as activation of anti-inflammatory pathways (Dombrowski et al., 2011, Pütsep et al., 2002).

1.1.2.2 Natural antibodies

Natural antibodies (NAb) are germline encoded immunoglobulins primarily produced by the B1 subpopulation of B lymphocytes and target epitopes that are not required to have been detected prior (Savage and Baumgarth, 2015). NAb

have a low affinity to a range of well-characterised self-and foreign antigens. Foreign antigen binding to NAb promote a variety of immune responses including promotion of antigen immunogenicity, recruitment of complement proteins, antigen opsonisation and initiation of FcR-mediated phagocytosis, (Benatuil et al., 2005, Chen et al., 2009, Panda and Ding, 2015) (Zhou et al., 2013). Low affinity binding to epitopes is due to minimal N-nucleotide insertions and hypermutations compared to adaptive immunity-derived antibodies, allowing nonlethal self-recognition for host-microbe homeostasis (Avrameas, 2016, Reyneveld et al., 2020). This illustrates the integration of the innate immune system for antipathogenic roles and its constant role in tissue homeostasis.

1.1.2.3 Pentraxins

Pentraxins are a superfamily of serum-phase PRRs characterised by the structure of the first discovered, C-reactive protein (CRP) (Du Clos and Mold, 2004). The family consists of two subgroups. Short pentraxins contain a Creactive protein with a serum amyloid P component, whereas long pentraxins consist of neuronal pentraxins 1-4, and a pentraxin receptor, with both families sharing a common c-terminal domain and discoid structure formed by pentameric complexes (Du Clos and Mold, 2004, Wang et al., 2020). Binding to a PAMP or DAMP such nuclear autoantigens allows long and short pentraxins to promote macrophage-mediated opsonisation and phagocytosis of apoptotic and pathogenic cells through interaction with Fc receptors (Mold et al., 2001, Mold et al., 2002).

1.1.2.4 Complement

Complement proteins are highly regulated serum proteins that result in a complex cascade that can target both pathogenic and infected host-derived cells for lysis, inflammation, and opsonisation (Merle et al., 2015). Activation is achieved through classical, alternative, and mannose binding lectin pathways, all resulting in convertase-induced cleavage of C3 leading to the cleavage of C5 and formation of C5b deposition and common terminal pathway activation (Merle et al., 2015). This induces the formation of the membrane attack complex and a pore, causing cell death even in parasites due to osmotic flux (Hoover et al., 1984).

1.1.3 Innate cell-mediated immunity

Non-myeloid cells like keratinocytes employ rapid innate immune responses as previously described. However, innate immunity through myeloid and lymphoid cells provides an elevated response against extracellular pathogens, infected and dead cells, as well as the ability to activate the adaptive immune system (Elliott et al., 2009, Ito et al., 2013, Lee et al., 2007). Recognition of PAMPs and DAMPs by these cells are conducted by a range of PRRs including TLRs, Fcγ receptors, and CLRs (Geijtenbeek and Gringhuis, 2009, Guilliams et al., 2014, Hoppstädter et al., 2010).

1.1.3.1 Myeloid cells

Macrophages

Macrophages are derived from circulating blood monocytes through differentiation stages resulting in common macrophage and DC precursor (MDP) and mature into macrophages either polarised towards a M1-like inflammatory or M2-like anti-inflammatory phenotype (Fogg et al., 2006, Yunna et al., 2020). Differentiation is dependent on stimuli at the site of infection for example, LPS drives a M1 phenotype whilst IL-4 drives M2 polarisation (Sica and Mantovani, 2012). M1 macrophages are characterise by overexpression of CD80, CD86, and CD68 (Cutolo et al., 2022, Wijesundera et al., 2014). Due to their immune promoting phenotype, M1 macrophages are associated with antipathogenic and tumour-suppressive responses (Boutilier and Elsawa, 2021). Upon PRR recognition, M1 responses include expression of strong proinflammatory cytokines (IL-6, TNF, and IFN-B) and chemokines (CCL2, CXCL10, and CXCL11), and increased antigen presentation after phagocytosis due to upregulation of MHC-I/II (Martinez and Gordon, 2014). On the other hand, M2 macrophages are characterised by expression of CD163 and CD206 receptors among others (Wang et al., 2017). M2 macrophages are associated with tissue healing, tolerance to self-antigens as the expression of immunosuppressive cytokines like IL-10 (Siqueira Mietto et al., 2015). Macrophage polarisation highlights its phenotypic plasticity needed for both phagocytosis and priming of the adaptive immune system as well as dampening inflammation for wound healing.

Neutrophils

Neutrophils are the most abundant leukocyte with approximately $1x10^{11}$ produced daily during bone marrow haematopoiesis and are regarded as the first responders of innate cell-mediated responses (Borregaard, 2010, Rosales, 2018). Upon activation, neutrophils have a variety of responses including phagocytosis, degranulation, and release of nuclear material known as neutrophil extracellular traps (NETs) (Mayadas et al., 2014). NETs consist of chromatin fibres containing granule-derived antimicrobial peptides and enzymes including neutrophil elastase, cathepsin G, and myeloperoxidase, resulting in binding and degradation of bacteria (Brinkmann et al., 2004). Whilst this destroys the neutrophil, most pathogens are neutralised by phagocytosis and granule secretion (Lee et al., 2003, Othman et al., 2021). Unfortunately, the effectiveness of these effectors can promote autoimmune diseases as cytokine and chemokine cascades induce inflammation and NET-induced damage of host-cells (Fu et al., 2021).

Dendritic cells

Dendritic cells develop from four groups of bone marrow progenitors resulting in DC precursor cells that circulate and differentiate into the three major DC subsets (Breton et al., 2015). Upon migration to sites of inflammation via CCR2-mediated chemotaxis, DCs recognise PAMPs from bacteria, viruses, parasites, and fungi with a plethora of PRRs including TLRs and CLRs (Lundberg et al., 2014, Serbina et al., 2008). The type of PRR activated modulates the type of signaling induced to surrounding cells, tailoring immune activation to specific pathogens (Lundberg et al., 2014). Antigen uptake also allows DCs to bridge the innate and adaptive immune systems via antigen presentation to CD4+ and CD8+ T cells via MHC-II and MHC-I, respectively (Jongbloed et al., 2010). DC signaling is also to specifies immune responses. For example, DCs highly express type-I interferons (IFN-I) in response to viral infection, promoting T cell survival and T_H1 differentiation which further promote DC responses through differentiation (Santini et al., 2000, Agnello et al., 2003).

1.1.3.2 Innate Lymphoid cells

Innate lymphoid cells (ILCs) are characterised by lymphoid morphology of CD127 and CD161 expression, but lack of surface receptors found on immune cells including NK (CD16), DCs (CD123), and T cells (CD3, TCRαβ, and TCRδ) (Bernink et al., 2017). ILCs consist of helper ILC subfamilies; ILC1, ILC2, and ILC3, which produce T helper (T_H) 1-associated cytokines (IFN-y and TNF-α), T_H2-associated cytokines (IL-5 and IL-13), and T_H17-associated cytokines (IL-17 and IL-22), respectively (Serafini et al., 2015). Alternatively, cytotoxic ILCs express CD94 and eliminate malignant- and pathogen-infected cells, producing cytokines and chemokines to recruit further immune cells to the site of infection (Krabbendam et al., 2021). Circulating ILCs allow tissue specific responses through differentiation into cytokine producing (ILC1-3) or a cytokine-producing cytotoxic cells (cytotoxic ILC) (Lim et al., 2017).

Natural killer (NK) cells account for 10-15% of peripheral blood mononuclear cells and are responsible for killing viral-infected and cancerous cells through multiple effector mechanisms (Jurisić, 2006). NK cells are characterised by the less prevalent and immature $CD56^{bright}CD16^{-}$ subset and the mature $CD56^{dim}CD16^{+}$ subset which have increased perforin expression (Chan et al., 2007). Host cells are targeted when MHC-I expression is lost, often induced by viral infection or cancerous phenotypes, resulting in loss of inhibitory NK signals (Kim et al., 2005). As well as a lack of MHC-I, NK cells also require recognition of stress related molecules, leading to granule exocytosis and death ligands that promote proapoptotic genes such as TNF-α in the target cell (Martínez-Lostao et al., 2015).

NK cells also secrete cytokines and chemokines upon activation to modulate innate and adaptive immune responses (Fauriat et al., 2010). Furthermore, NK cells promote DC recruitment and maturation to prime the adaptive immune system (Walzer et al., 2005).

1.1.4 Pattern recognition receptors

1.1.4.1 Toll like receptors

First described to have anti-pathogen activity in *Drosophila melanogaster*, Toll like receptors (TLRs) have since been extensively researched (Lemaitre et al., 1996). There are ten human (TLR1-TLR10) and thirteen (TLR1-TLR13) mouse TLR homologs that detect a range of pathogens including viruses, bacteria, fungi, and parasites, due to localisation in a range of cellular compartments including lysosomes, endosomes, and plasma membrane, as seen in ***Table 1*** (Akira et al., 2006). Each TLR binds to a PAMP specific to a general type of pathogen such as TLR4 affinity to LPS, a component of Gram-negative bacteria, whereas TLR3 binds to dsRNA to detect viruses during replication (Alexopoulou et al., 2001, Chow et al., 1999). As seen in ***Figure 2***, TLRs are characterised by three structural domains including N-terminal domain (NTD) containing leucine-rich repeats (LRR) responsible for ligand binding, a transmembrane region, and a cytoplasmic Toll/interleukin-1 receptor (IL-1R) homologous region (TIR) signaling domain. The TIR domain can interact with five adaptor proteins for signal transduction including MyD88 (Myeloid differentiation factor 88), MAL/TIRAP (MyD88-adaptor-like/TIR-associated molecule), TRIF (Toll-receptor-associated activator of interferon), TRAM (Toll-receptor-associated molecule), which activate protein kinases and transcription factors to induce inflammatory effects (Beutler, 2004). The fifth adaptor, HEAT/Armadillo motif protein (SARM) is a TLR3 and TLR4 regulator via TRIF inhibition (O'Neill and Bowie, 2007).

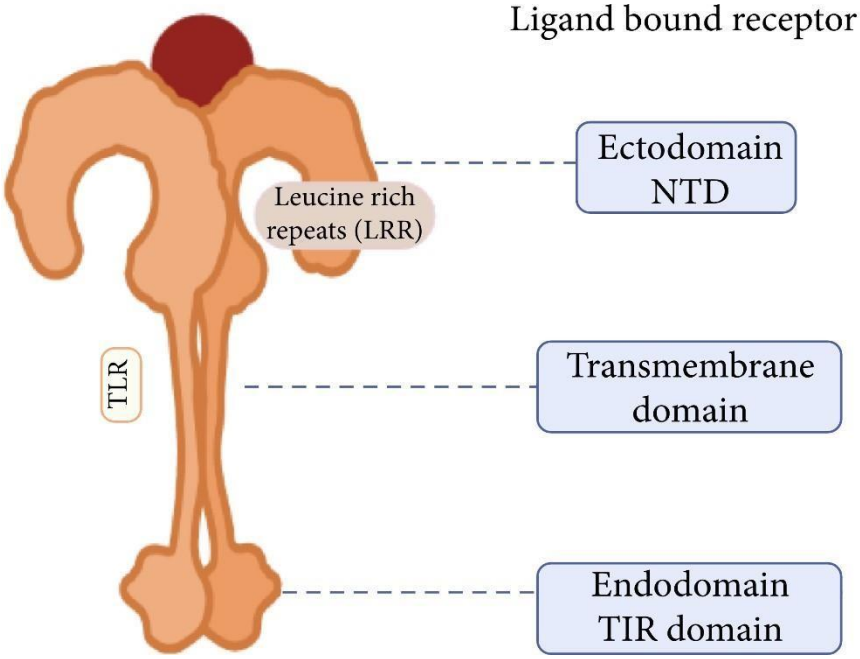

Figure 2. Schematic of a ligand bound TLR.

Consisting of an extracellular N-terminal domain (NTD), transmembrane domain, and an intracellular toll-IL-1 receptor (TIR) homologous domain. Modified from Sameer and Nissar, (2021).

Table 1. Overview of TLR homolog localisation, expression in immune cells, ligands, and cytokine response.

Table modified from Martinsen et al., (2020).

Localisation	TLR Homolog	Cell Type	Ligand	Outcome
Extracellular Membrane	TLR1	Monocytes Dendritic cells T cells	- Lipopeptides from bacteria and mycobacteria	Proinflammatory cytokines
	TLR2	Monocytes Macrophages Dendritic cells	- Components from the cell wall of grampositive bacteria - Glycoprotein from viruses - Zymosan from fungi	Proinflammatory cytokines
	TLR4	Monocytes Dendritic cells	- Lipopolysaccharides from gram-negative bacteria - Envelope components of respiratory syncytial virus (RSV)	Proinflammatory cytokines and IFNs
	TLR5	Monocytes T cells	- Flagellin from flagellated bacteria	Proinflammatory cytokines

	TRL6	Monocytes Macrophages B cells	- Lipopeptides from Mycoplasma	Proinflammatory cytokines
	TLR10	B cells	- Ligands from Listeria - Ligands from Influenza A	
Endosomal	TLR3	Dendritic cells	- Viral doublestranded RNA	Proinflammatory cytokines and IFNs
			- Self-RNA from damaged cells	
	TLR7	Plasmacytoid dendritic cells B cells	- Viral singlestranded RNA	Proinflammatory cytokines and IFNs
	TLR8	Monocytes Dendritic cells	- Viral singlestranded RNA - Bacterial RNA	
	TLR9	Plasmacytoid dendritic cells B cells	- CpG containing DNA from bacteria and viruses	Proinflammatory cytokines and IFNs
			- Self-DNA from damaged cells - Hemozoin from Plasmodium Falciparum	

TLR signaling can induce MyD88-dependent pathways through MyD88IRAK4IRAK2 complex death domain (DD) formation, which recruits and activates an E3 ubiquitin ligase, tumour necrosis factor receptor-associated factor 6 (TRAF6) (Gorjestani et al., 2012). As illustrated by ***Figure 3***, TRAF6 induces the nuclear import of NF-κB via K63-linked polyubiquitination of TAB2/3, activation of TAK1 kinase, formation of the IKK complex and inhibition of the Iκβα NF-κB complex inhibitor (Wang et al., 2001). NF-κB then promotes the expression of proinflammatory cytokines and chemokines such as TNF, IL-1B, IL-6, IL-12, and CCL2 (Deng et al., 2013, de Winther et al., 2005). Alternatively, TRIF-dependent signaling pathways activated by TLR 3 and TLR4 primarily induces expression of type-I IFNs via IRF3 (Akira and Takeda, 2004).

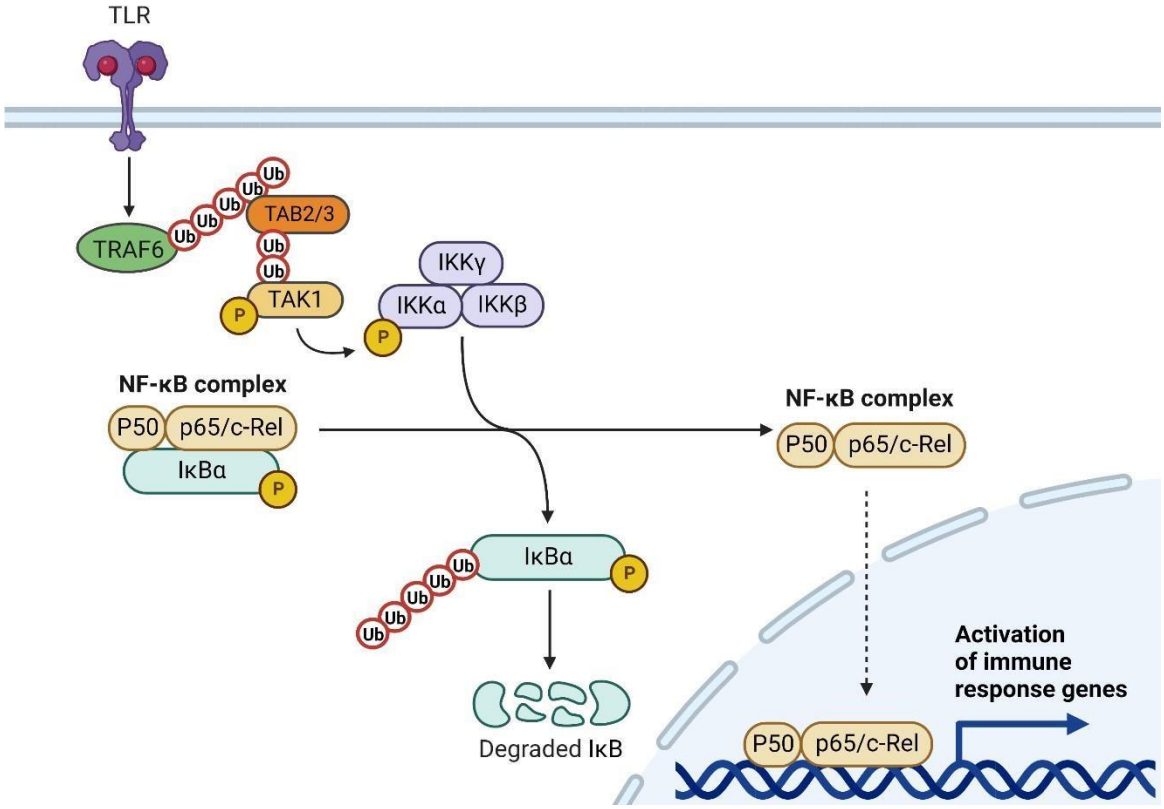

Figure 3. TLR induced activation of NF-κB through tumour necrosis factor receptor-associated factor 6 (TRAF6).

Upon ligand stimulation, MyD88 recruits TRAF6 to assemble an MyD88 signalling complex where TRAF6 acts as an E3 ubiquitin ligase that catalyses the formation of K63-linked polyubiquitin chains for association, polyubiquitination, and activation of TAB2/3. Activated TAB2/3 recruits and activates TAK1 through K63linked polyubiquitin chain formation, allowing the formation of the IKK

complex, marking Iκβα for degradation via phosphorylation, allowing the nuclear import of NF-κB. Figure Created with BioRender.

1.1.4.2 RIG-I-like receptors

RIG-I-like receptors (RLRs) are a class of PRR that take advantage of the viral lifecycle requirement to release a genome consisting of RNA within an infected cell. The class consists of retinoic acid-inducible gene I (RIG-I), melanoma differentiation associated gene 5 (MDA5), and laboratory of genetics and physiology 2 (LGP2). RIG-I was the first RLR to be isolated and is a part of the DExD/H box-containing RNA helicase family, containing two N-terminal caspase recruitment domains (CARDs) and a C-terminal helicase domain capable of initiating an IFN-I response, in response to RNA transfection (polyI:C) or 5'triposphate capped RNA exposure via the activation of NF-κB and IRF-3 (Hornung et al., 2006, Kato et al., 2005, Yoneyama et al., 2004). MDA5 is another dsRNA receptor containing CARD and helicase domains, however, recognises longer dsRNA strands (>2kb) whereas RIG-I detects shorter strands (Approximately 25bp) (Takahasi et al., 2008, Kato et al., 2008, Kato et al., 2006). Although LGP2 contains the helicase domain found in RIG-I and MDA5, it does not contain an N-terminal CARD and instead is a regulator of RIG-I and MDA5 mediated signaling via its repressor domain (RD) (Saito et al., 2007). However, recent evidence indicates LGP2 promotes the MDA5-mediated IFN response to HCV (Hei and Zhong, 2017).

RLR activation induces a conformational change that induces CARD-CARD homotypic association, allowing interaction with the ISP-1 adaptor protein known as mitochondrial antiviral-signaling protein (MAVS), and recruits TRAF2/3/6 which activate NF-κB as previously described, and IRF3/7 via the non-canonical IKK complex, as illustrated in ***Figure 4*** (Chariot et al., 2002, Oganesyan et al., 2006, Perry et al., 2004, Saito et al., 2007). The IRF3/7 induced IFN-I is a potent antiviral response targeting viral replication, and initiates cell-mediated responses during the initial stages of bacterial infections. (McNab et al., 2015, Yan and Chen, 2012). The autocrine and paracrine signalling of IFN-I and subsequent expression of interferon stimulated genes (ISG) employs mechanisms to prevent every step of viral replication including IFITM expression to block viral entry,

TRIM5α to disrupt retrovirus uncoating and target viral proteins for proteasomal degradation, and Mx GTPases to recognise nucleocapsids and block nuclear import (Liao et al., 2019, Haller et al., 2015, Ganser-Pornillos and Pornillos, 2019).

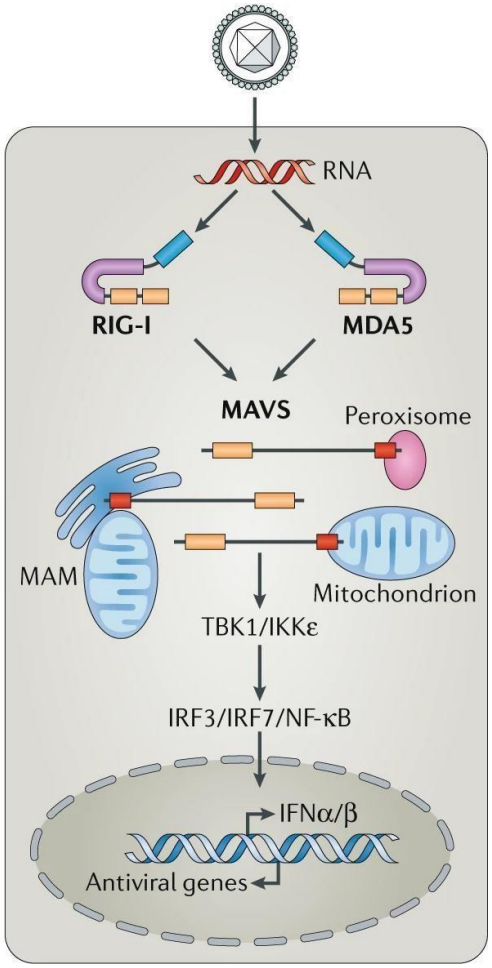

Figure 4. RLR driven IFN-I response following viral RNA sensing. *Recognition of viral RNA induces a conformational change in RIG-I/MDA5, exposing and multimerising CARDS and interactions with mitochondrial antiviral signaling protein (MAVS).The MAVS signalling protein is anchored to mitochondria and mitochondrial-associated membranes (MAMs), and relays signals to TBK1 and IKKε which induce nuclear import of IRF3, IRF7, and NF-κB. Figure modified from Rehwinkel and Gack, (2020).*

1.1.4.3 Nucleotide-binding oligomerisation domain-like receptors (NLR)

NOD-like receptors (NLRs) are a diverse family of cytosolic PRR expressed on both immune and non-immune cells (Hisamatsu et al., 2003, Ogura et al., 2001, Tada et al., 2005, Voss et al., 2006). The PRR family consists of NLRA, NLRB,

NLRC, NLRP and NLRX subfamilies that all contain a central NACHT nucleotide binding domain (NBD) for oligomerisation, and leucine-rich repeats (LRR) for ligand binding, with each subfamily contrasting by N-terminal CARD, acidic transactivation, pyrin domain (PYD), caspase domain, and baculoviral inhibitory repeat-like domains (Harton et al., 2002, Ting et al., 2008). NLRs detect a range of pathogens and PAMPs from peptidoglycans found in gram-negative and grampositive bacteria to RNA from viruses depending on the subfamily (Benko et al., 2008, Chamaillard et al., 2003, Thomas et al., 2009). Upon LRR-ligand binding, LRR undergoes a conformational change and oligomerisation, allowing recruitment of PYD containing proteins via CARD (Inohara et al., 1999, Ojcius and Saïd-Sadier, 2012). CARD induces the activation of NF-kB via Rip2 recruitment, JNK, and MAPK activation, as well as IFN-I expression through TRAF3 activation (Bertin et al., 1999, Hsu et al., 2007, Watanabe et al., 2010). This response drives the expression and processing of IL-1a, IL-1B, and IL-18, promoting recruitment of neutrophils, macrophages, cytosolic activity of NK cells, and inflammasome formation, and cell death (Franchi et al., 2009, Viganò et al., 2015).

1.1.4.4 C-type Lectin receptors

Like TLRs, C-type lectin receptors (CLRs) are a large family of PRR that detect PAMPs from a range of pathogens and are found on a variety of cells including macrophages, dendritic cells, epithelial cells, and hepatocytes (Azad et al., 2014, Choteau et al., 2016, Jiang et al., 1995). The CLRs family consists of soluble receptors, type 1, and type 2.

Although the soluble class of CLRs only consists of mannose-binding lectin (MBL), it is a crucial for recognition of PAMPs on the surface of microorganisms, providing a broad first-line defence both intracellularly and extracellularly (Kalia et al., 2021). MBL has shown to bind to sugar groups, phospholipids, nucleic acids, and non-glycosylated proteins it has shown to bind to bacteria, viruses, fungi, and protozoa (Kahn et al., 1996, Neth et al., 2000, Saifuddin et al., 2000, Townsend et al., 2001). Upon activation on the extracellular surface of pathogens, MBL induces the activation of the complement, aids in phagocytosis, and modulates inflammatory responses (Neth et al., 2000).

Type 2 CLRs consist of four subfamilies with proinflammatory and anti-inflammatory roles. Both Dectin-1 and Dectin-2 bind to B-glycan and mannans, respectively (Brown et al., 2003, Feinberg et al., 2017). Upon activation, Dectin1 and Dectin-2 induces reactive oxygen species (ROS) and potassium efflux, promoting the activation of NLRP3 inflammasome and NF-kB (Hernanz-Falcón et al., 2009, Sancho and Reis e Sousa, 2012). DC-SIGNs are expressed by DCs and recognise multiple pathogens including *Mycobacterium tuberculosis*, *M. leprae*, *Candida albicans*, and measles (Gringhuis et al., 2007). Ligand binding also induces NF-kB acetylation via Raf-1 and IL-10 expression for antiinflammatory effects upon TLR-induced activation (den Dunnen et al., 2009, Gringhuis et al., 2007). Like DC-SIGN, DNGR-I has a regulatory role upon activation with exposed B-actin from damaged and dying cells by dendritic cells and F-actin from yeast (Ahrens et al., 2012, Zhang et al., 2012).

1.2 DNA sensing

1.2.1 Canonical STING pathway

STING canonical pathway can be activated through pathogen derived double stranded DNA (dsDNA) or DAMPs in the form of cytosolic self-DNA via cyclic GMP-AMP synthase (cGAS), as illustrated in ***Figure 5***. cGAS has been a unique PRR that is not found in the previous four classes described and binds in a DNA sequence independent but DNA-length dependent manner (Sun et al., 2013). Although cGAS has shown to binds to dsDNA with a 1:1 stoichiometry through a single binding site however, more recent studies have shown cGAS forming a 2:2 complex with dsDNA through two binding sites, indicating activation through dsDNA induced oligomerisation (Donovan et al., 2013, Li et al., 2013, Zhang et al., 2014).

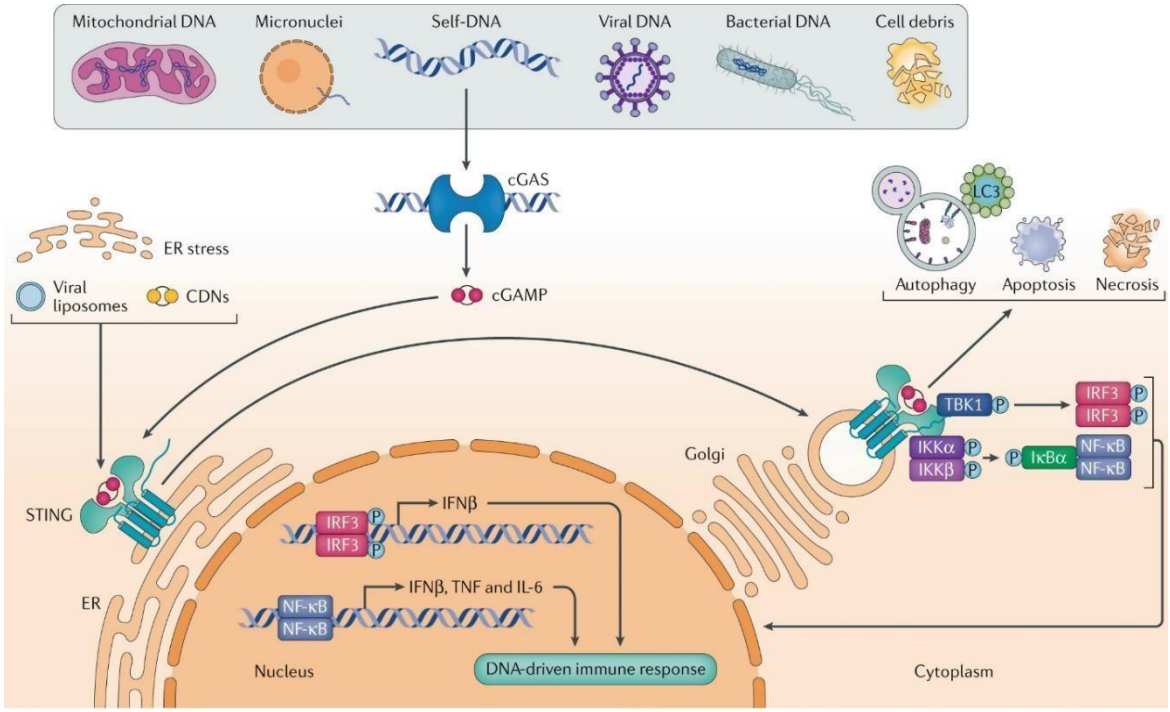

Figure 5. Cytosolic DNA sensing by the cGAS-STING pathway.

Cytosolic dsDNA from a variety of sources, acting as a PAMP or DAMP activates the canonical STING pathway through the binding of cyclic GMP-AMP synthase (cGAS). This initiates the production of the secondary messenger, cyclic GMPAMP (cGAMP), which binds to inactive STING within the endoplasmic reticulum (ER). cGAMP binding to STING allows its activation and translocation to ER-Golgi intermediate compartments where recruitment of TANK-binding kinase 1 (TBK1) and IkB kinase (IKK) induces the phosphorylation of interferon regulatory factor 3 (IRF3) and the NF-κB inhibitor IκBα, respectively. Nuclear import of IRF3 is the primary response whilst cytokines and chemokines expressed by NF-kB is induced to a lesser extent. IRF3 induces the expression of type-I interferons such as IFN-B. IFN-I expression can induce numerous responses such as inflammasome activation, senescence, and autophagy. Figure modified from Motwani et al., (2019b).

The structure of human (h) cGAS and its binding interactions with DNA have been difficult to resolve compared to other species. The difference between hcGAS and mouse (m) cGAS for example was known to be significant as Sun at al., 2013 found hcGAS produced significantly less of its secondary messenger, 2'3'-cyclic guanosine monophosphate-adenosine (cGAMP), and subsequent IFNB induction than mcGAS. This is now known to be due to h-cGAS showing

enzymatic sensitivity depending on DNA length. A high-resolution x-ray crystallography structure of hcGAS binding to 17bp DNA was achieved through K187N and L195R substitutions (Zhou et al., 2018). This showed similar overall structure to previous human and non-human cGAS, consisting of an N-terminal lobe of B1-B9 central- twisted B-sheets flanked by a1-a7 helices and a compact a8-a12 helix bundle with a zinc binding motif at the C-terminal lobe (Zhang et al., 2014). As well as two DNA binding sites (site-A and site-B) in each of the enzymes two monomers (Zhou et al., 2018). As highlighted by blue residues in ***Figure 6***, L195R stabilises DNA interaction by increasing positive charge of the A-site DNA binding surface, whilst K187N interacts with the DNA phosphate backbone, allowing Y215 to reposition and stabilise the active site loop for nucleotide coordination (Zhou et al., 2018). These substitutions also highlighted h-cGAS enzymatic sensitivity depending on DNA length. As WT hcGAS with K187 and L195 was not able to bind to DNA <45bp, showing tolerance to small DNA fragments unlike mcGAS (Zhou et al., 2018). This relatively low sequence homology highlights the difficulties of using non-human cGAS and other STING components for understand mechanisms behind diseases and testing therapies.

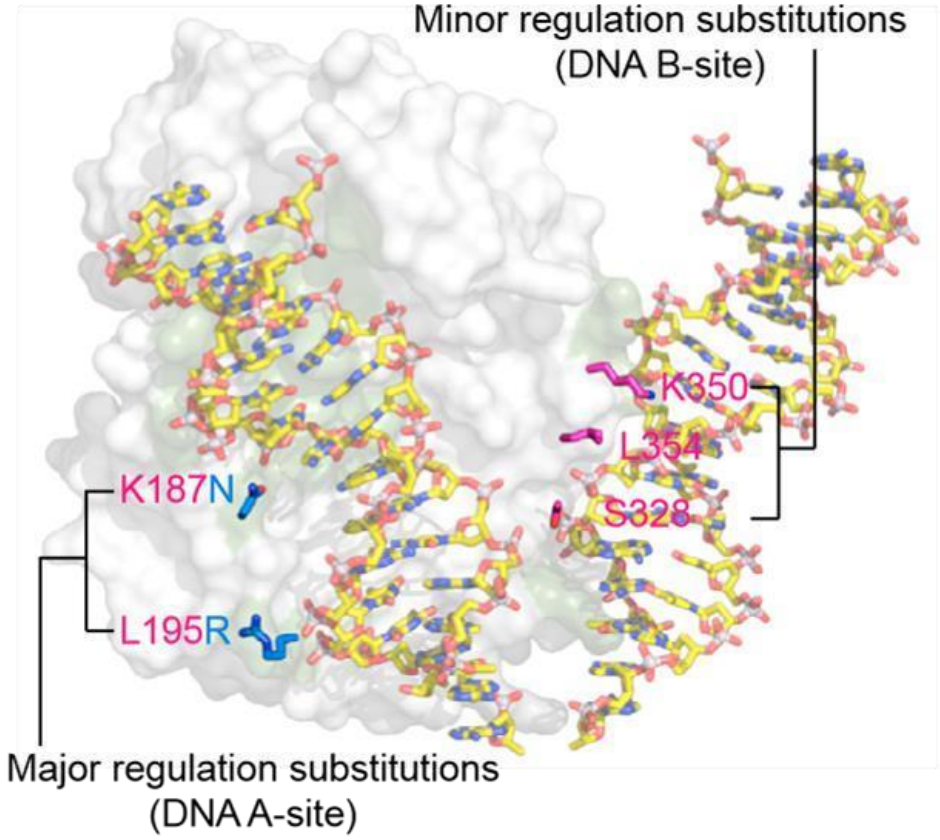

Figure 6. Human cGAS-bound-DNA complex.

The diagram highlights interactions at A-site and B-site. Blue coloured residues highlighting positions of K187N and L195R mutations within the DNA A-site and have a major role in binding interactions and enzyme activity. Magenta coloured residues in the DNA B-site have a minor role. Figure modified from Zhou et al., (2019).

The conformational change induced by dsDNA binding derives from the activation loop as G212 and S213 move inward whilst V218 and K219 shift away to rearrange and activate the nucleotidyltransferase domain within the catalytic site, as illustrated in ***Figure 7*** (Zhang et al., 2014). Once cGAS is allosterically activated by dsDNA, the production of cGAMP from cyclic guanosine monophosphate (GMP) is achieved through a two-step process firstly, through catalysis of a linear 2' -5'-linked dinucleotide then a 3'-5' phosphodiester linkage (Ablasser et al., 2013). Production of cGAMP not only allows diffusion and activation of STING via autocrine signalling but can activate STING in surrounding cells via gap junctions (Sundararaman and Barbie, 2018).

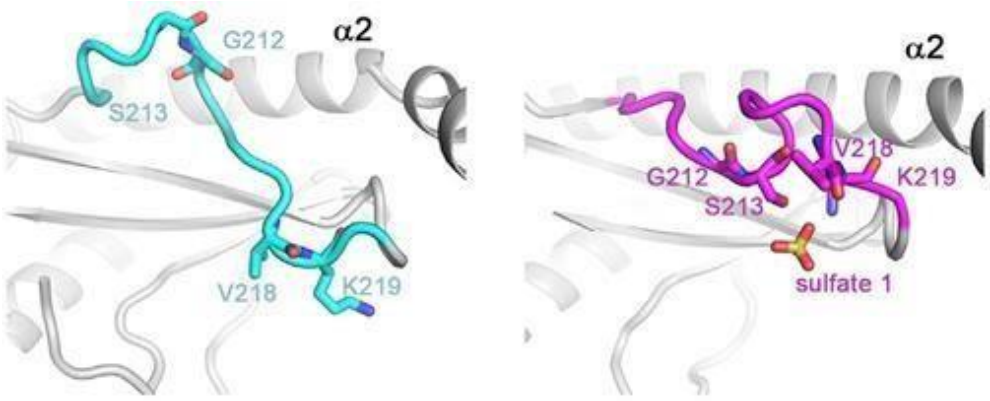

Figure 7. Ligand induced conformation changes of the cGAS activation loop and active site.

Structures shown show the inward shift to active site and bound sulphate ion from residues G212 and S213 whilst V218 and K219 shift away from the ligand. Conformational changes induced by bound sulphate imitate the binding to DNA. Figure modified from Zhang et al., (2014).

A STING monomer consists of four transmembrane helices (TM1-TM4) with the connector helix extending extracellularly to the connector loop where the ligand binding pocket and active site can be found, as illustrated by ***Figures 8b*** and ***8d***.

Unbound human STING resides anchored to the ER as a dimer at approximately 80 kDa with domain swap architecture as the monomers are interlocked which is illustrated in ***Figure 8C*** (Shang et al., 2019). Whilst inactive, STING is autoinhibited by its C-terminal tail (CTT) which interacts and blocks the polymerisation interface, preventing formation of STING polymers and its trafficking to ER-Golgi intermediate compartments (Ergun et al., 2019). Although STING is activated by cGAMP, it is also activated by other cyclic dinucleotides (CDNs) such as cyclic-di-GMP and c-di-AMP that act as a PAMPs as they are bacterial signalling molecules that can activate STING directly in mice (Burdette et al., 2011). cGAMP binding to the ligand binding domain (LBD) formed by the TM2-TM3 linkers and connector helix induces a closed conformation around cGAMP (Shang et al., 2019). This induces a 180° rotation of the LBD driven by unwinding of connector loops and exposure of the polymerisation interface previously blocked by the CTT, allowing polymerisation assisted by disulphide bridge formation between dimers and palmitoylation of cysteine residues (Mukai et al., 2016, Ergun et al., 2019, Shang et al., 2019). This allows STING trafficking via cytoplasmic coat protein complex II (COPII) and ADP-ribosylation factor (ARF) GTPases, and once at the Golgi undergoes post-translational modification needed for its activation (Dobbs et al., 2015, Gui et al., 2019, Mukai et al., 2016). STING activation is also promoted by interacting with the DNA binding protein IFI16 which shuttles out of the nucleus during infection and decreases DNA induced clustering of STING significantly in HaCaT keratinocytes if not present (Almine et al., 2017). Localisation at the Golgi allows interaction with a TBK1 dimer on the top of the STING cytosolic ligand-binding domain, which has been defined as a TBK1-binding domain at residues 369-377 in human STING (Zhang et al., 2019). Phosphorylation of STING by TBK1 at serine-366 allows IRF3 to bind to the CTT of STING and IRF3 is then phosphorylated due to proximity of TBK1 (Liu et al., 2015). P-IRF3 dimerises and undergoes nuclear import to induce IFNB expression, which promotes anti-viral responses via autocrine and paracrine signalling (Schneider et al., 2014).

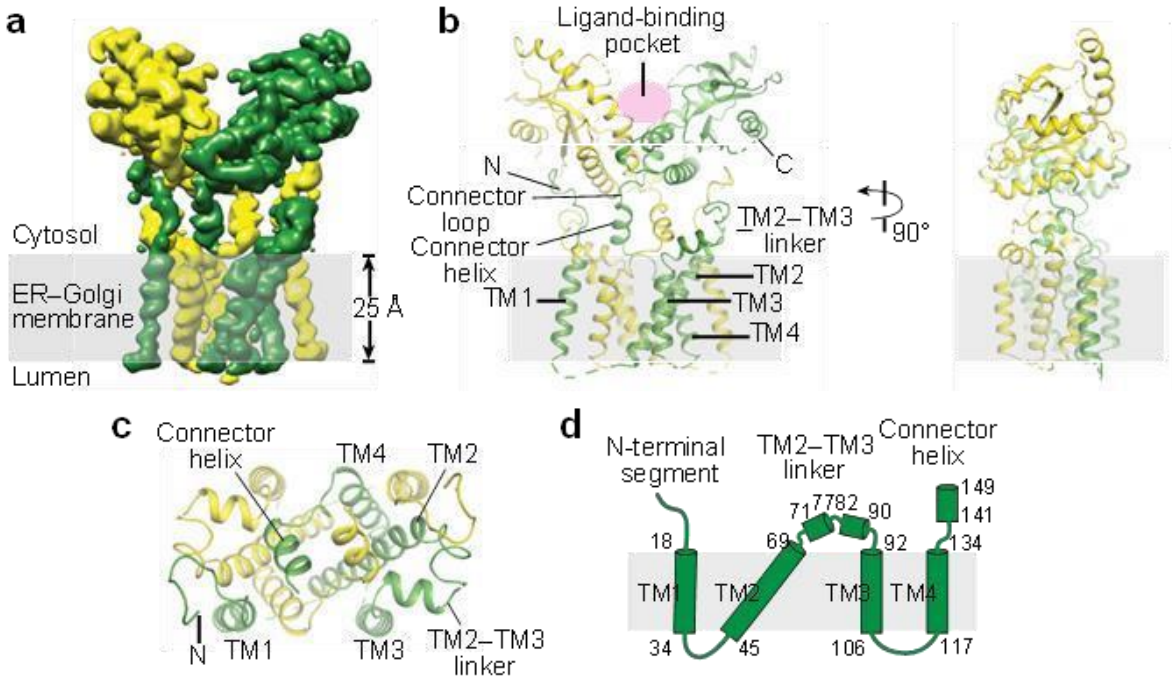

Figure 8. Structure of human STING in unbound state. ***a*** *cryo-EM horizontal view of a STING dimer.* ***b*** *Labelled cartoon representations of cryo-EM structure highlighting structural elements and location of ligand binding pocket.* ***c*** *cartoon representation of transmembrane region viewed from the cytosolic side.* ***d*** *topological diagram of a STING dimer consisting of transmembrane domains 1-4. Figure modified from Shang et al., (2019).*

1.2.2 Non-canonical STING pathway

The canonical STING pathway is pivotal for responding to infection after detection of cytosolic DNA but can also be activated by PAMPs in the form of micronuclei, a DNA damage biomarker, caused by chromatin leakage (Fenech et al., 2020). Alternatively, it was found that DNA damage could also induce STING activation in a cGAS-independent manner (Dunphy et al., 2018). The non-canonical pathway is initiated by two damage response factors as seen in ***Figure 9***. Upon a dsDNA break within the nucleus, poly (ADP-ribose)-polymerase-1 (PARP-1) assembles a nucleoplasmic signalosome, whilst ataxia telangiectasia mutated kinase (ATM) activates TRAF6, allowing its nuclear export and association to STING (Hinz et al., 2010).

Through etoposide-induced DNA damage, non-canonical activation of STING was observed independently of cGAS-cGAMP and led to a proinflammatory cell intrinsic immune response via NF-kB, with IRF3 activation to a lesser extent

(Dunphy et al., 2018). Like TRAF6, ATM also activates p53 via phosphorylation followed by its association to either HIN-A or HIN-B domains of IFI16 (Liao et al., 2011). Furthermore, TRAF6 has shown to bind to the CTT tail of zebrafish STING, specifically to a highly conserved PxExxD motif related to TRAF binding sites in human (de Oliveira Mann et al., 2019). This CTT has shown to directly recruit TRAF6 and activate NF-kB, however, is not found in human STING(de Oliveira Mann et al., 2019). Instead, IFI16 is needed to recruit TRAF6 to the STING complex in human HaCaT cells (Dunphy et al., 2018). Furthermore, IFI16 contains a PxExxD motif within an exposed loop of the HIN-B domain (Ni et al., 2016). This could be the TRAF6 binding domain with p53 still able to bind to the HIN-A domain but is yet to be confirmed. IFI16 is pivotal for non-canonical activation as a deletion of IFI16 prevents phosphorylation of the NF-κB subunit, P-p65, at residues S205, T254, S276, S281, S311 adjacent to its N-terminal and T435, S468, T505, S529, S535, S536, and S547 within the C-terminal transactivation domain (Hochrainer et al., 2013, Dunphy et al., 2018). The association of the p53-IFI16-TRAF6 catalyses the formation of K63-linked ubiquitin chains on STING (Dunphy et al., 2018). Although the consequence of STING polyubiquitination is not fully understood, ubiquitin chains allow the formation of complexes that include kinases such as TAB2/3 which contain ubiquitin-binding domains (Walsh et al., 2015). This could also explain localisation of TAK1 to STING. Importantly, TRAF6 polyubiquitinates TAB2/3 once localised to STING, allowing the recruitment of TAK1 and its activation through autophosphorylation (Xia et al., 2009). TAK1 then induces IKK complex formation via phosphorylation. The IKK complex then phosphorylates S32 and S36 of IκBα, targeting the protein for degradation and preventing its inhibition of NF-κB (Viatour et al., 2005).

Within the nucleus, NF-κB will drive expression of pro-inflammatory cytokines and chemokines including IL-1, TNF-a, IL-6, CCL2, and CCL20 (Dunphy et al., 2018). These inflammatory signals recruit innate immune cells such as macrophages which further promote an inflammatory environment through secretion of proteins such as TNF-α (Schlaepfer et al., 2014, Wang et al., 2014). Differentiation of anti-inflammatory immune cells is also downregulated as IL-6 inhibits formation of regulatory T cells (Bettelli et al., 2006). The non-canonical STING response also stimulates expression of repair factors and induction of homologous

recombination, promoting dsDNA break repair via BRCA1 complexes and interaction partners with p65 (Volcic et al., 2012, Wu et al., 2000). However, excess homologous recombination can promote genetic instability leading to tumorigenesis (Canitrot et al., 2004). Furthermore, NF-κB hyperactivation is associated with range of autoimmune diseases including rheumatoid arthritis and type 1 diabetes, highlighting the potential of innate immune responses to become highly pathogenic when dysregulated (Pai and Thomas, 2008).

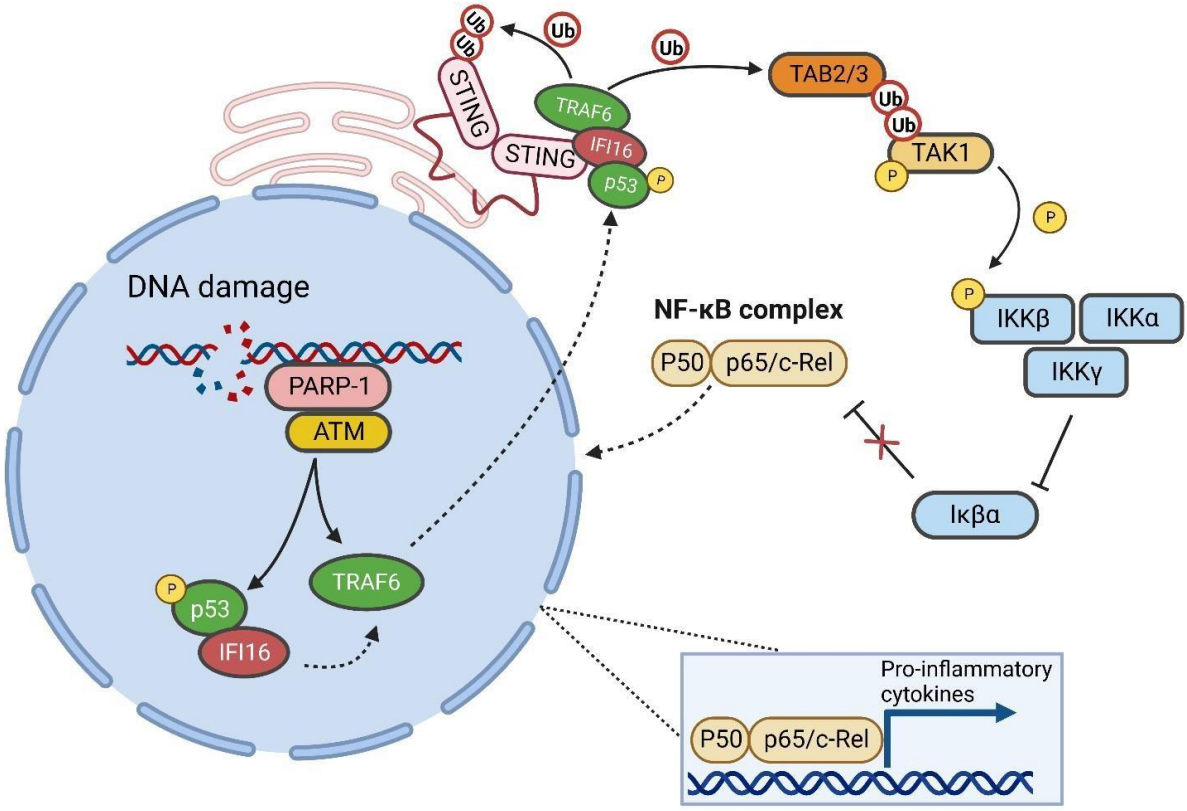

Figure 9. DNA damage-induced activation of the non-canonical STING pathway.

dsDNA breaks are sensed and activate PARP-1 and ATM, leading to the phosphorylation of p53 and activation of IFI16. P-p53 bound IFI16 and TRAF6 are exported to the cytosol. IFI16 binds to STING, allowing TRAF6 to polyubiquitinate STING and TAB2/3, allowing the localisation and activation of TAK1 kinase. TAK1 induces formation of the IKK complex through phosphorylation which inhibits the NF- κB inhibitor, IkBα. Created in BioRender.

1.3 STING associated vasculopathy with onset in infancy

First identified in 2014, STING associated vasculopathy with onset in infancy (SAVI) is a rare autoinflammatory disease with symptoms able to present as early as 1 day of age (Liu et al., 2014). The disease is driven by ligand-independent activation through gain-of-function mutations within the TMEM173 gene encoding STING, which are in either the connector helix loop (V147L, N154S, V155M, and V155R) or the polymerisation interface (G207E, R281Q, R284G, and R284S), as summarised by ***Figure 10*** (Keskitalo et al., 2019, Liu et al., 2014, Saldanha et al., 2018). Onset of the disease varies as early as from birth in more severe cases associated with connector helix loop mutations compared to 13 years of age with less severe polymerisation interface mutations (Alghamdi et al., 2020). SAVI is associated with a range of symptoms including systemic inflammation, skin lesions, fever, interstitial lung disease (ILD), and lung fibrosis leading to a premature death (Liu et al., 2014).

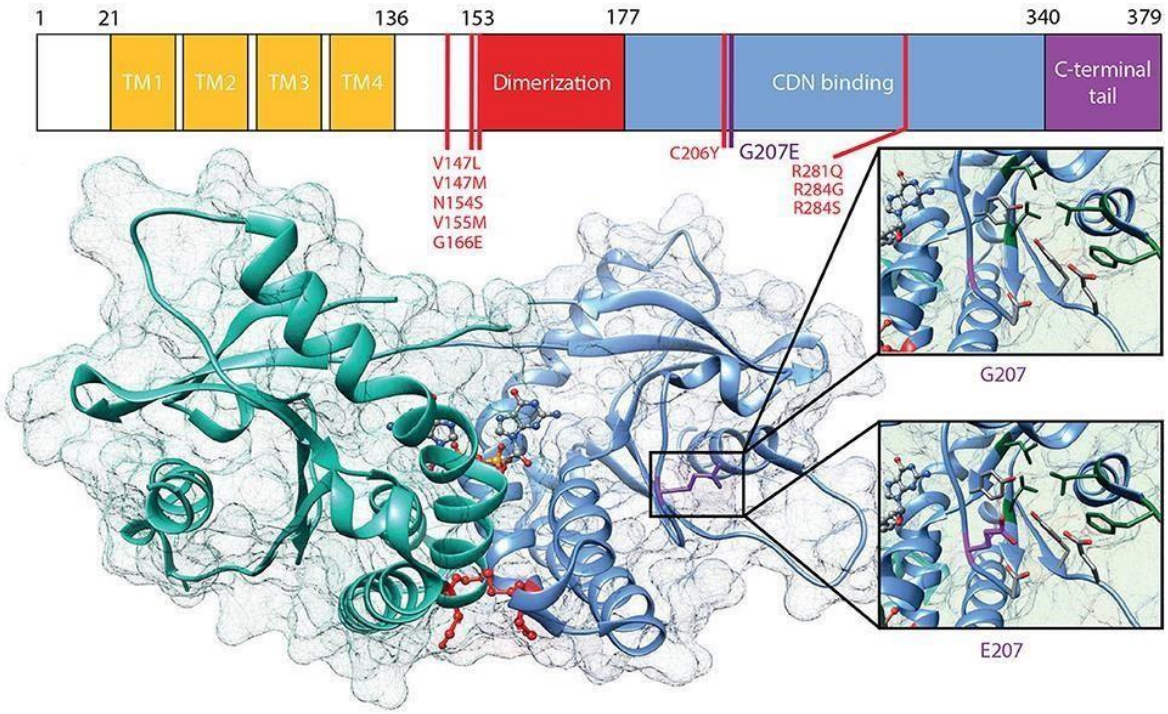

Figure 10. Locations of SAVI inducing mutations in correlation with the structure of STING.

SAVI-STING mutations in correlation with the structure of STING including transmembrane (TM), dimerisation, cyclic-di-nucleotide binding domain (CDN), and C-terminal tail are highlighted in red and purple residues. Figure modified from Keskitalo et al., (2019).

1.3.1 Signalling pathways responsible for SAVI

It was presumed that SAVI was induced by the canonical pathway due to heightened expression levels of IFN-I in SAVI patients and SAVI model cell lines independent of cytosolic DNA induced STING activation (Liu et al., 2014, Melki et al., 2017). However, generation of heterozygous mouse models including heterozygous STING N153S and knockout of IRF3 was able to establish IRF3independent severe combined immunodeficiency disease (SCID), T cell cytopenia, lung inflammation, hypercytokinemia, skin ulcerations, and premature death in mice expressing STING N153S combined with the IRF3 deletion in mouse models (Warner et al., 2017). As seen with previous H293T SAVI models, ISG expression was mildly upregulated via IRF3 however, its knock-out in mice shows IRF3 activation is not the primary cause of lung inflammation and skin disease. Instead, hypercytokinemia analysis of serum from STING v155M mice showed significantly higher levels of cytokines associated with NF-κB activation including TNF-a, MIP-1a, and MIP-1B (Warner et al., 2017).

Another study involving N153S and V154M SAVI-STING mouse models established a significantly higher proinflammatory expression profile associated with NF-κB gene targets such as IL-6, TNF-a, RANTES, MCP1, GCSF, and MIP1B (Motwani et al., 2019a). Furthermore, STING V154M, the mouse equivalent of V155M in human STING was the most potent mutant in this model (Motwani et al., 2019a). Finally, this led to generation STING V154M with knockout of IRF3, and STING V154M with knockout of IFNAR mouse models, which showed no significant difference in disease severity or outcome compared to the mice with STING V154M (Motwani et al., 2019a). Like the previous study, this also concludes that IRF3 and IFN-I has a minimal role in disease outcome, with NF-κB showing stronger activity instead. However, deletion of NF-κB has not yet been performed in this context.

1.3.2 Current treatments

Upon expression, IFN-I bind to IFN-I receptors and activate Janus activated kinase (JAK)-signal transducer and activator of transcription (STAT) complexes which promote expression of ISGs (Platanias, 2005). Currently, inhibition of IFNI

stimulated pathways via JAK inhibitors are most used to prevent disease progression but have varied and often unsustainable outcomes (Wang et al., 2021).These IFN inhibitors have been administered on a range of SAVI inducing mutations. Intriguingly, the first homozygous variant of TMEM173 mutations at R281W in exon 7 of the STING1 gene was identified in siblings aged 13 and 7 years old, resulting in increased serum IFN-B levels (Alghamdi et al., 2020). Surprisingly, this homozygous variant was less severe compared to other heterozygous variants such as V155M and N154S. With administration of Ruxolitinib, a JAK1/2 inhibitor, successfully decreasing ISG levels and preventing disease progression (Alghamdi et al., 2020). A more severe case from an N154S TMEM173 variant initially presented with ILD and skin lesions at 6 months and was diagnosed with SAVI at 10 months of age due to high ISG levels (Balci et al., 2020). Ruxolitinib was not effective from diagnosis leading to administration of Baricitinib, another JAK1/2 inhibitor, 5 months later resulting in fewer cutaneous manifestations and respiratory symptoms within 2 months (Balci et al., 2020).

Ruxolitinib, was administered to 3 children with unspecified TMEM173 variants but initially displayed increased ISG levels (Frémond et al., 2016). The JAK2/3 inhibition resulting in a general improvement with almost complete resolution of cutaneous lesions and a major improvement in pulmonary function after 16 months of treatment (Frémond et al., 2016). However, two of the patients eventually required lung transplantation with the other only showing a long-term mild improvement (Frémond et al., 2016). This case study overall showed despite significant clinical improvement initially, the inability to completely inhibit IFN-I signalling only warranted variable reduction of ISG expression and modest fold changes in expression in immune-related genes unable to prevent chronic lung inflammation. Unfortunately, ILD can lead to fibrotic lung disease resulting in respiratory failure, limiting patients to higher risk treatments. This includes lung transplantation which has led to humoral rejection and death one year after transplantation and was not able to prevent another patient succumbing to multiple organ dysfunction syndrome (Clarke et al., 2020, Frémond et al., 2021).

As previously described drug trials show IFN-I inhibition is highly variable and not a reliable long-term resolution. Overall, drug inhibition of JAK1/2 by Ruxolitinib, Baracitinib, and Tofacitinib have been more effective than JAK1/3 inhibitors (Hadjadj et al., 2021). This could be explained by partial blocking of NF-κB as to JAK2 activation can lead to IL-33-induced Iκβα degradation, implying noncanonical STING activation could be responsible for SAVI (Funakoshi-Tago et al., 2011). Regardless of the STING pathway responsible, a treatment targeting upstream components of the disease would be more effective than downstream components such as JAK and NF-κB.

1.3.3 Use of STING inhibitors

Clinical use of STING inhibitors is in initial stages but are promising. Firstly, a peptide STING antagonist known as ISD017 has shown to inhibit downstream effects of STING including autophagy, apoptosis, and expression of IFN-I and inflammatory cytokines in cultured mouse H293T and RAW264.1 macrophage cells (Prabakaran et al., 2021). H-151 is an antagonist that has been shown to irreversibly inhibits STING through covalently binding to C91 in mice and HEK293T cells (Haag et al., 2018). The use of the H-151 showed inhibition of IFN-I, and unlike the Tofacitinib JAK1/2 inhibitor, was able to decrease upstream levels of IFN-B (Deng et al., 2020). Administration of H-151 in mice displayed a short half-life in serum due to quickly interacting with STING whilst displaying high selectivity in human cells as well (Haag et al., 2018). This makes H-151 a promising candidate for inhibition of STING in SAVI models. However, the use of STING inhibitors on cell lines with SAVI-STING and effect on non-canonical STING signalling via TRAF6 have not been tested and published to date.

1.4 Aims

This project will investigate signalling outputs caused by a STING hyperactivating mutation found in SAVI patients. The aims of this project are:

- To determine hyperactivation of the proinflammatory non-canonical STING signalling pathway in STING V155M expressing human HaCaT keratinocytes.
- To determine whether proinflammatory signalling cascades in HaCaT cells are suppressed by STING inhibition.

This will be achieved by molecular techniques including immunoblotting, immunofluorescence confocal microscopy, quantitative Real Time-PCR, ELISA, and H-151 inhibition of STING. Through the use of these techniques, we aim to determine which signalling cascades induce hyper-activation of the innate immune system in SAVI-STING-expressing skin cells. This project could provide insight into potential novel treatment targets for a rare, yet life limiting and incurable condition.

2 Materials and methods

2.1 Cell culture

HaCaT cell lines were cultured in Gibco Dulbecco's Modified Eagle's Medium (DMEM) (Life technologies) with 10% Fetal Bovine Serum (FBS) (Sigma) and 50µg/mL Gentamicin (Life technologies) at 37°C in 5% CO2.

2.2 Buffers used

Table 2. Buffers used throughout this project.

1X PBS	1mM Na_2HPO_4 137mM NACl 1.8mM KH_2PO_4 2.7mM KCl Adjust to pH 7.4
Phospholysis Buffer	50mM Tris-HCL (pH 7.5) 1mM EDTA (pH 8) 1mM EGTA 1% (v/v) Triton X-100 1mM Sodium Orthovanadate 50mM Sodium Fluoride 5mM Sodium pyrophosphate 10mM β-glycerophosphate, disodium salt 0.27M Sucrose Adjust to pH 7.5
3X SDS Sample Buffer	62.5mM Tris-Cl pH 6.8 2% (w/v) SDS 10% (v/v) Glycerol 0.1% (w/v) Bromophenol Blue Adjust final volume to 50ml with dH_2O
Stacking Gel Tris Buffer	0.5M Tris Base Adjust pH to 6.8
Resolving Gel Tris Buffer	1.5M Tris Base Adjust pH to 8.8

1X Running Buffer	25mM Tris Base 192mM Glycine 1% (v/v) SDS
1X Transfer Buffer	25mM Tris Base 192mM Glycine
1X TBS	5mM Tris Base 15mM Tris HCl 150mM NaCl Adjust pH to 7.6
TBST	0.1% Tween-20 in TBS
Reagent Diluent	1% BSA in PBS
ELISA Washing Buffer	0.05% Tween 20 in PBS

2.3 Expression of STING V155M

To activate Lenti-X Tet-one Inducible expression, WT STING knockout, STING V155M HaCaT cells were treated with 1μg/ml doxycycline for at least 24 hours to prior to treatment with etoposide or analysis of STING expression via immunoblotting or immunofluorescence confocal microscopy.

2.4 DNA transfection

Transfection of herring testis (HT) DNA was conducted with Lipofectamine 2000 (Invitrogen) at a ratio of 1:1. WT HaCaT cells were transfected with 10μg/ml HT DNA or Lipofectamine 2000 as a control.

2.5 Etoposide treatment

DNA damage was induced in HaCaT cells with 50μM etoposide with DMSO as a control.

2.6 H-151 treatment

To inhibit STING, HaCaT cells were treated with 4µg/ml (InvivoGen) H-151 for 24h. To inhibit STING V155M, H-151 was added at the same time as doxycycline in SAVI cells, 24h prior to further treatments. DMSO was used as a control.

2.7 Immunoblotting

HaCaT cells were seeded in 6-well plates at $3x10^5$ cells/ml. After treatment HaCaT cells were incubated in 1.5ml phospholysis buffer for 30 minutes on ice with lysate scraped into Eppendorf tubes and centrifuged at 13,000 rpm for 10 minutes at 4°C. Lysates were denatured with SDS sample buffer at 99°C for 10 minutes.

Table 3. Reagents for 12% acrylamide SDS-PAGE gel.

	dH_2O	40% Acrylamide	1.5M Tris	10% SDS	10% APS	TEMED
Resolving Gel (12%)	4.4ml	3.0ml	2.5ml	0.1ml	50µl	5µl
	dH_2O	40% Acrylamide	0.5M Tris	10% SDS	10% APS	TEMED
Stacking Gel (4%)	1.9ml	0.3ml	0.75ml	30µl	30µl	3µl

Denatured lysates with SDS sample buffer were loaded into a 12% SDS-PAGE gel in a Mini-PROTEAN Tetra Vertical Electrophoresis Cell (Bio-Rad) and run for 1.5 hours at 120V. Proteins were transferred to PDVF or nitrocellulose membranes (Cytiva) with a semi-dry electroblotting transfer pack for 1 hour at 0.1 Amp per SDS-PAGE gel. Membranes were blocked with 3% BSA (Sigma)/TBST for 1 hour at room temperature before probing with primary antibodies at a dilution of 1:1000 then incubated overnight at 4°C. Membranes were washed 3X 5 minutes in TBST and probed with secondary antibodies (Anti-rabbit IgG, HRPlinked Antibody or Anti-mouse IgG, HRP-linked Antibody from Cell Signalling) at a dilution of 1:6000 for 2-3 hours at room temperature. Membranes were developed with HRP substrate with ECL (Clarity™ Western ECL substrate from Bio-Rad) for 5 minutes under Chemiluminescent mode Chemidoc (Bio-Rad).

2.8 Immunofluorescence confocal microscopy

HaCaT cells were seeded in a 24-well plate at a concentration of $3x10^5$ cells/ml on coverslips. After treatment, cells on coverslips were washed in PBS and fixed in cold methanol (for imaging STING) or 4% paraformaldehyde (PFA) (for imaging NF-κB and IRF3) for 10 minutes. Cells were then washed 3X 5 minutes in PBS then permeabilised in 0.5% Triton-X/PBS for 12 minutes at room temperature. Then coverslips were washed for 3X 5 minutes in PBS and blocked in 5% FCS, 0.2% Tween-20 /PBS (STING) or 5% BSA, 0.2% Tween-20 /PBS (NF-κB/IRF3) for 1 hour at room temperature before probing with primary antibodies at a dilution of 1:600 in blocking buffer overnight at room temperature. Cells were 3X washed for 5 minutes in PBS then probed with Alexa Fluor® 488 goat anti-mouse IgG (Life technologies) or Anti-rabbit IgG Fab2 Alexa Fluor (R) 594 (Cell Signaling) secondary antibodies at a dilution of 1:1500 In blocking buffer in darkness for 3h at room temperature. Coverslips were 3X washed 5 minutes in PBS then mounted onto slides in MOWIOL containing DAPI, left to dry for 1 hour, and sealed. Slides were stored in darkness at 4°C.

2.9 Antibodies Used throughout project

Table 4. of antibodies utilised throughout project.

Target	Species	Company	Catalogue number
STING	Rabbit	Cell Signaling	D2P2F
IFI-16	Mouse	Santa Cruz	1G7
NF-kappaB p65	Rabbit	Cell Signaling	D14E12
NF-kappaB p65	Mouse	Cell Signaling	L8F6
P-NF-kappaB p65 (S536)	Rabbit	Cell Signaling	93H1
IRF-3	Rabbit	Cell Signaling	D6I4C
B-actin	Mouse	Sigma Aldrich	A2228
Anti-mouse-HRP	Horse	Cell Signaling	7076
Anti-rabbit-HRP	Goat	Cell Signaling	7074

Anti-rabbit Alexa Fluor 594	Goat	Cell Signaling	8889
Anti-mouse Alexa Fluor 488	Goat	Thermo Fisher Scientific	A11029

2.10 Quantitative Real-Time PCR

RNA extraction was conducted with the E.Z.N.A.® MicroElute Total RNA kit by Omega Bio-Tek. Cell media was removed, and cells washed twice in PBS and incubated in TRK lysis buffer for 5 minutes whilst being incubated on ice then transferred into Eppendorf tubes with equal volume of 70% ethanol. The sample was transferred into HiBind Mini Column in a collection tube and centrifuged at 10,000 xg for 1 minute with filtrate discarded. Columns were washed with RNA Wash Buffer I and centrifuged at 10,000 xg for 1 minute with filtrate discarded. DNase and DNase digestion buffer (1.5µl and 73.5µl per tube) was added to samples for 15 minutes at room temperature. Samples were left in RNA Wash Buffer I for 2 minutes at room temperature and centrifuged at 10,000 xg for 1 minute with filtrate discarded, followed by two more washes with RNA Wash Buffer II and centrifugation with filtrates discarded. Columns were centrifuged at maximum speed until dry and eluted in 50µl nuclease free water in Eppendorf tubes after centrifugation. RNA concentrations were measured using a Nanodrop 2000C spectrophotometer and samples were diluted to the same concentration with nuclease free water.

cDNA synthesis was conducted with the advance iScript cDNA synthesis kit by Bio-Rad. All samples and plates were kept on ice for cDNA synthesis. cDNA master mix (2µl Reaction Buffer and 0.5µl Reverse Transcriptase per tube) was added to tubes with 100ng of RNA per tube with final volume adjusted to 10µl with RNase free water. Tubes were incubated in an Eppendorf Master Cycler for 20 minutes at 46°C and 1 minute at 95°C with cDNA stored at -20°C.

cDNA samples (10µl) were diluted in 30µl nuclease free water then added to iQ SYBR® Green-primer master mix (5µl Fast SYBR™ Green from Thermo Fisher

Scientific and 1µl Primer mix consisting of 1:20 forward and reverse primers in nuclease free water) for genes desired in a 96 well PCR plate, totalling to 10µl per well. The qRT-PCR was conducted in a Bio-Rad CFX 96 Real-Time PCR detection system at the following settings:

Holding stage (1 cycle)

95°C for 600 seconds

Cycling stage (40 cycles)

95°C for 15 seconds
60°C for 1 minute

Melting curve stage (1 cycle)

95°C for 15 seconds

60°C for 1 minute

95°C for 15 seconds 60°C

for 15 seconds

Ct values from RT-PCR were presented as averages of biological triplicate samples with standard deviations shown as error bars.

Table 5. Primers utilised for RT-PCR.

Target sequence	**Forward**	**Reverse**
CCL2	TCAGCCAGATGCAATCAATGCC	GCTTCTTTGGGACACTTGCTG
CCL20	AACCATGTGCTGTACCAAGAGT	AAGTTGCTTGCTTCTGATTCGC
IL-6	CAGCCCTGAGAAAGGAGACAT	GGTTCAGGTTGTTTTCTGCCA
GAPHD	CTCCTGTTCGACAGTCAGCC	ACCAAATCCGTTGACTCCGAC

2.11 ELISA

ELISA for detection of CCL20 secretion was performed with bio-techne R&D systems Human CCL20/MIP3 alpha DuoSet® ELISA kit. Concentrations of

capture antibody, standards, detection antibody, and HRP-streptavidin were prepared according to manufacturer's instructions with reagent diluent. The 96 well ELSIA plate had capture antibodies (2μg/ml) added overnight at room temperature. The plate was 3X washed with washing buffer and blocked with reagent diluent for 2 hours at room temperature. Samples (undiluted HaCaT supernatant) and standards (from 2000pg/ml to 31.2pg/ml diluted 2-fold) were added to appropriate wells and were incubated overnight at room temperature and 2X washed. Detection antibody (50ng/ml) was added for 2 hours at room temperature and 2X washed. HRP-streptavidin was then added and kept in darkness at room temperature for 20 minutes. The plate was 2X washed then substrate solution was added to wells for 20 minutes at most before stop solution (H_2SO_4) was added. Absorbances were measured by a Tecan infinite 200 PRO Microplate reader at 450nm with wavelength correction of 540nm. Absorbances were generated as averages of biological triplicate samples from the standard curve, with standard deviations shown as error bars.

3 Results

3.1 Selective expression of STING V155M in HaCaT cells

To establish selective expression of STING knockout human HaCaT keratinocytes reconstituted with STING V155M (SAVI cells), doxycycline was added to activate Tet-One induced gene expression. As seen in ***Figure 11A***, doxycycline treatment induced expression of STING V115M, as highlighted by the green arrow. Whereas no doxycycline (0h) lacked this intense band therefore did not induce observable expression of STING V155M via immunoblotting, which is also confirmed by densitometry in ***Figure 11B***. STING V155M appeared as a heavier band compared to WT STING due to the attachment of a HA-tag, adding further confirmation of its selective expression. ***Figure 11A*** also showed the presence of IFI16 in both HaCaT cell lines, a component needed for both canonical and non-canonical STING activation (Almine et al., 2017, Dunphy et al., 2018). Furthermore, the two red arrows highlight likely phosphorylated STING bands from WT HaCaT cells that were transfected with cytosolic DNA (HT DNA) for 2h and 4h. The decrease in WT STING intensity is another indication of canonical activation as the protein is turned over following activation, resulting in a higher band. Notably etoposide treatment does not induce as much STING phosphorylation as the higher STING band is not as intense, indicating an alternative post translational modification for non-canonical activation.

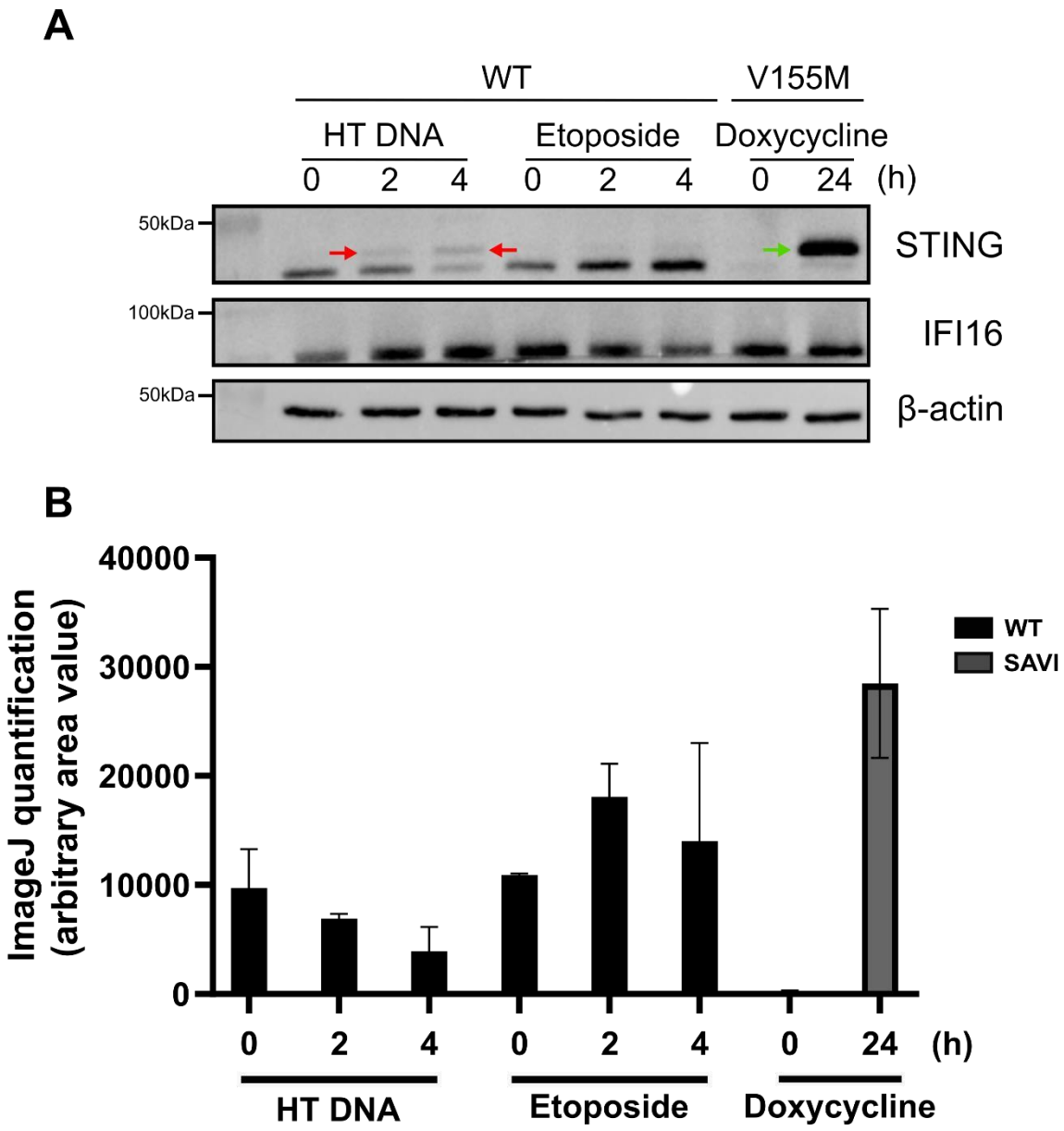

Figure 11. Selective expression of STING V155M in HaCaT cells. ***(A)*** *Western blotting and* ***(B)*** *densitometry analysis of STING expression normalised to B-actin expression. WT HaCaT cells (lanes 1-6) were transfected with 10µg/ml herring testis DNA or treated with 50µM etoposide for times indicated. HaCaT STING V155M cells (lanes 8 and 9) were treated with 1µg/ml doxycycline to induce STING V155M expression. Proteins levels of STING and IFI16 were visualised by immunoblotting with anti-STING and anti-IFI-16 antibodies. Phosphorylated STING and STING V155M are highlighted by red and green arrows, respectively (n = 2).*

Immunofluorescence confocal microscopy confirmed the expression of WT and doxycycline-induced STING V155M in HaCaT cells. The top row of ***Figure 12*** shows expression of WT STING (red) in untreated HaCaT cells with fluorescence throughout the cytosol evenly distributed. Alternatively, doxycycline-induced STING V155M expression in the middle row of ***Figure 12*** clearly showed red fluorescent clustering of STING V155M close to the nucleus which is a sign of activation due to STING oligomerisation. As expected, untreated SAVI cells did not appear to express STING V155M as shown by the lack of red fluorescence (***Figure 12***, bottom row). Both ***Figure 11*** and ***Figure 12*** confirmed doxycycline induced expression of STING V155M in SAVI cells.

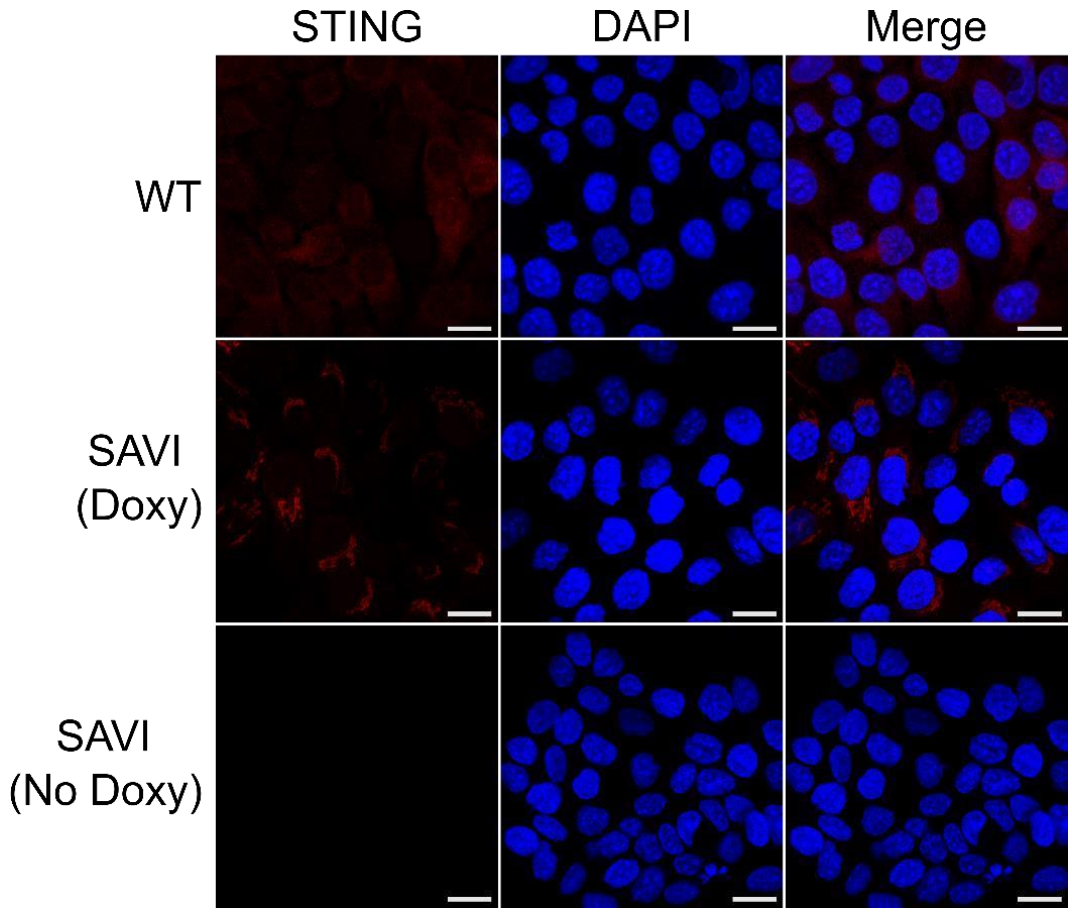

Figure 12. Selective expression of STING V155M and comparison of clustering to WT STING.

WT HaCaT cells or cells expressing STING V155M (SAVI Doxy) were grown on coverslips and treated with 1μg/ml doxycycline for 24h or left untreated.

Coverslips were stained for DNA (DAPI, blue) and STING (red). Scale bar, 20μm.

3.2 Constitutive hyperactivation of NF-κB in STING V155M cells

Figure 13 showed the effects of etoposide-induced DNA damage in WT HaCaT and SAVI cells. The NF-κB subunit p65 is phosphorylated at S536, resulting in Pp65 band intensity and implies non-canonical STING activation. Interestingly, Pp65 band intensity of the doxycycline-treated SAVI DMSO control appeared to be the same compared to with etoposide for an hour. However, it was clear to see that under all conditions P-p65 band intensity of doxycycline treated SAVI cells was significantly greater than WT HaCaT cells. Furthermore, as seen quantified in ***Figure 13B***, P-p65 intensity of the doxycycline treated SAVI DMSO control was greater than that of WT HaCaT cells treated with etoposide for an hour, implying constitutive hyperactivation of the non-canonical pathway induced by the V155M STING mutation.

Phosphorylation of p65 also appeared to be occurring in untreated SAVI cells in all conditions resembling doxycycline treated SAVI cells but at a lower intensity. This was surprising due to the lack of observable STING expression shown in ***Figure 13A***.

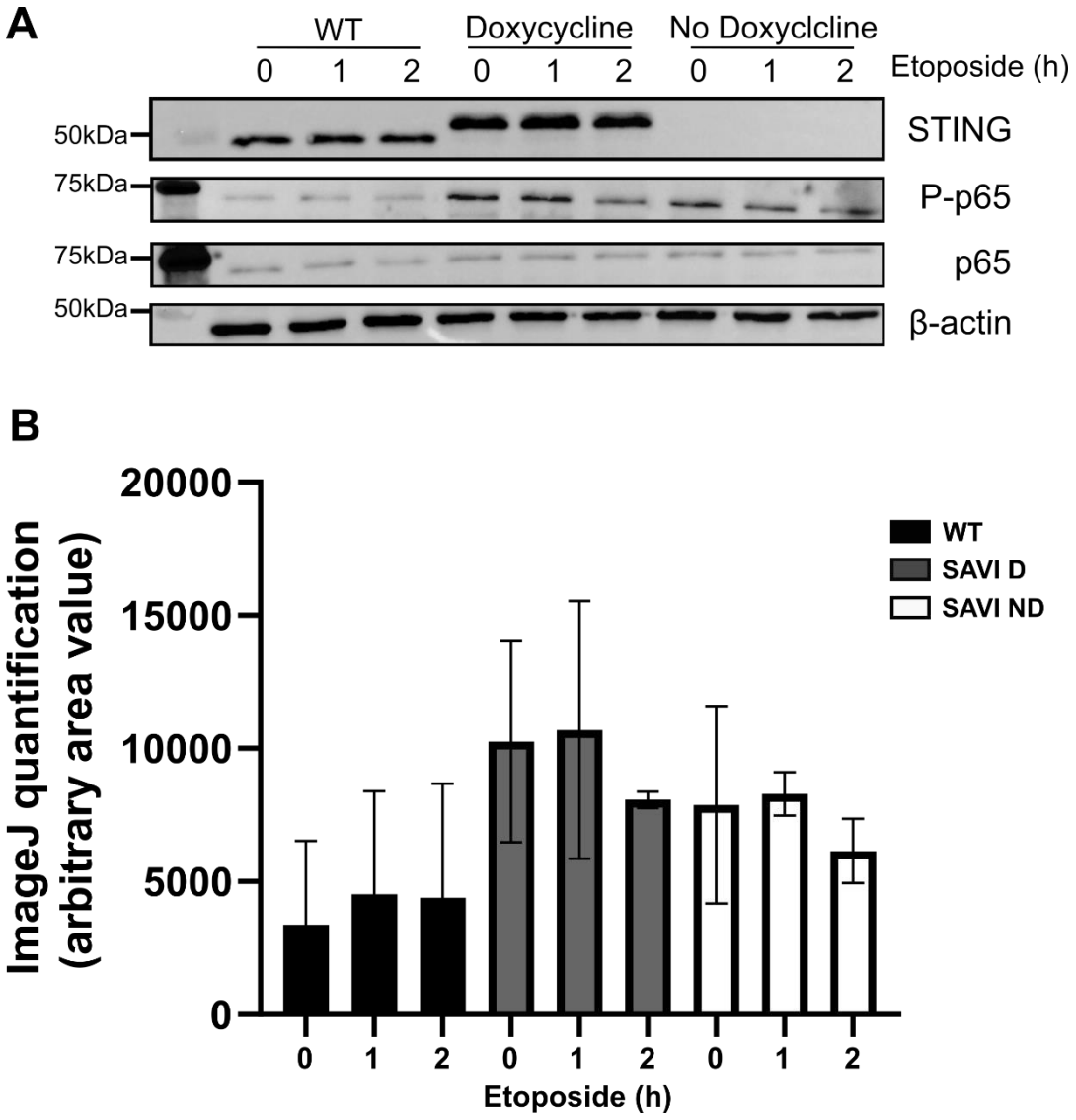

Figure 13. Constitutive hyperphosphorylation of p65 in STING V155M expressing cells.

(A) *Western blotting and* ***(B)*** *densitometry analysis of P-p65 levels normalised to B-actin expression. WT HaCaT and HaCaT STING V155M cells were treated with 50μM etoposide for times indicated or DMSO for 2h. HaCaT STING V155M cells were treated with 1μg/ml doxycycline for 24h where indicated. Proteins levels of STING, p65, and P-p65 were visualised by immunoblotting with anti-STING (D2P2F), anti-NFkappaB p65 (L8F6), and anti-P-NF-kappaB p65 (S536) antibodies (n = 2).*

Although phosphorylation of p65 is an indicator of NF-κB activation, immunofluorescence confocal microscopy (***Figure 14***) was used to confirm activation through detection of its nuclear localisation. As expected, nuclear localisation of NF-κB and IRF3 in WT HaCaT cells was not present in the DMSO

control, with NF-κB nuclear uptake increasing significantly after etoposide (1h and 2h) treatment, highlight by red arrows in ***Figure 14A***. ***Figure 14A*** also showed H-151-induced inhibition of NF-κB nuclear localisation in cells pre-treated with H151 (24h) followed by etoposide (1h) compared to etoposide treatment alone. This shows inhibition of the DNA damage induced non-canonical STING signalling pathway.

Interestingly, SAVI cells treated with doxycycline (SAVI doxy) and DMSO (***Figure 14B***) showed nuclear localisation of NF-κB and IRF3 as indicated by red and green arrows, respectively even in the absence of etoposide treatment. Furthermore, transcription factor translocation was suppressed by H-151 however, modest levels of NF-kB nuclear import remained. ***Figure 14B*** indicated a stronger response to etoposide from SAVI doxy cells compared to WT HaCaT cells (***Figure 14A***) indicated by higher levels of NF-κB and IRF3 nuclear localisation, notably after 2 hours of etoposide treatment. Like WT HaCaT cells, NF-κB nuclear import in SAVI doxy cells was decreased when etoposide was added to H-151 treated cells.

Surprisingly, SAVI cells that were not treated with doxycycline (***Figure 14C***) showed the same trends as SAVI doxy cells but with NF-κB and IRF3 nuclear induction at comparatively lower level, suggesting there may have been some residual SAVI-STING expression.

WT HaCaT **(A)**

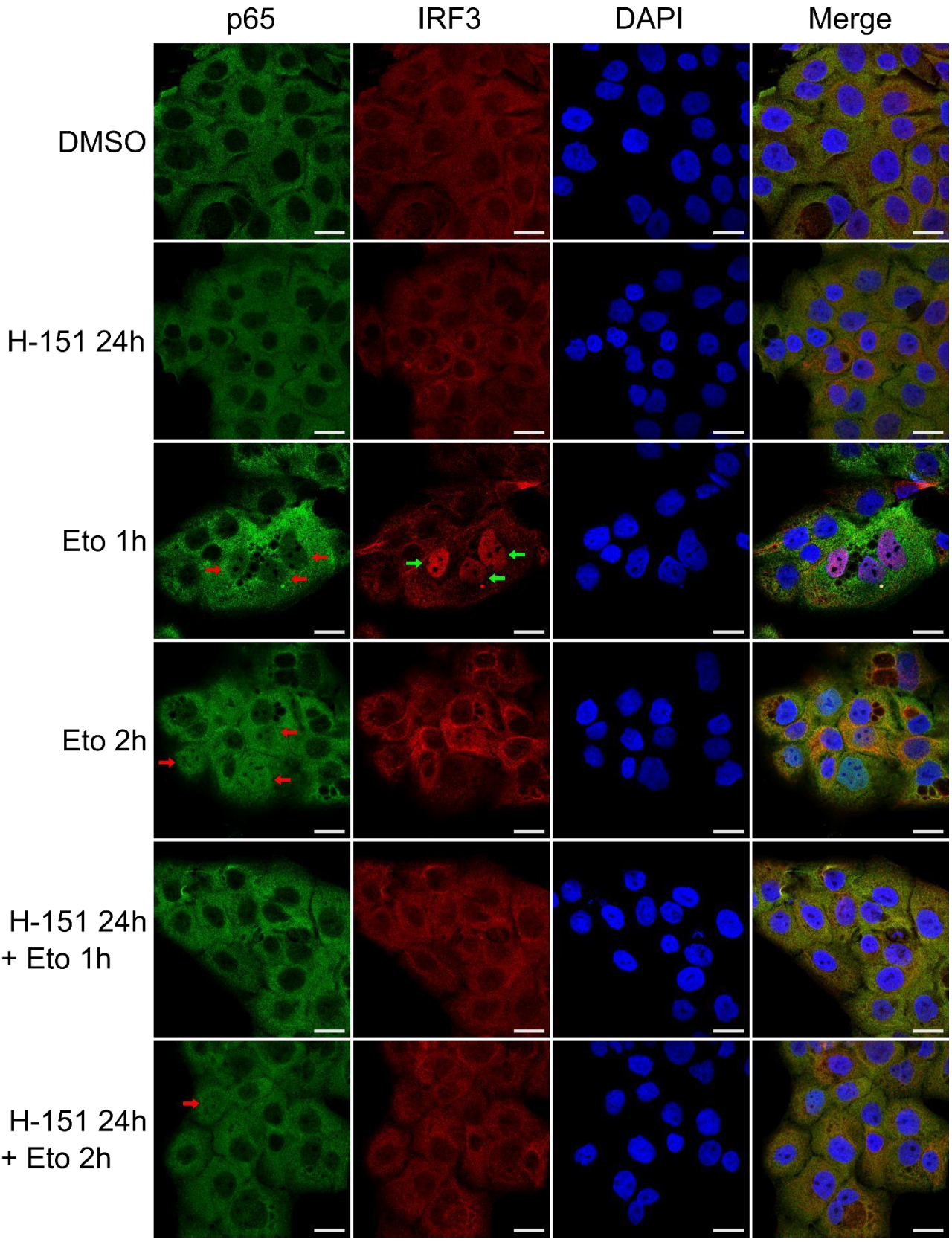
p65
IRF3
DAPI
Merge
DMSO
H-151 24h
Eto 1h
Eto 2h
H-151 24h
+ Eto 1h
H-151 24h
+ Eto 2h

HaCaT STING V155M with doxycycline **(B)**

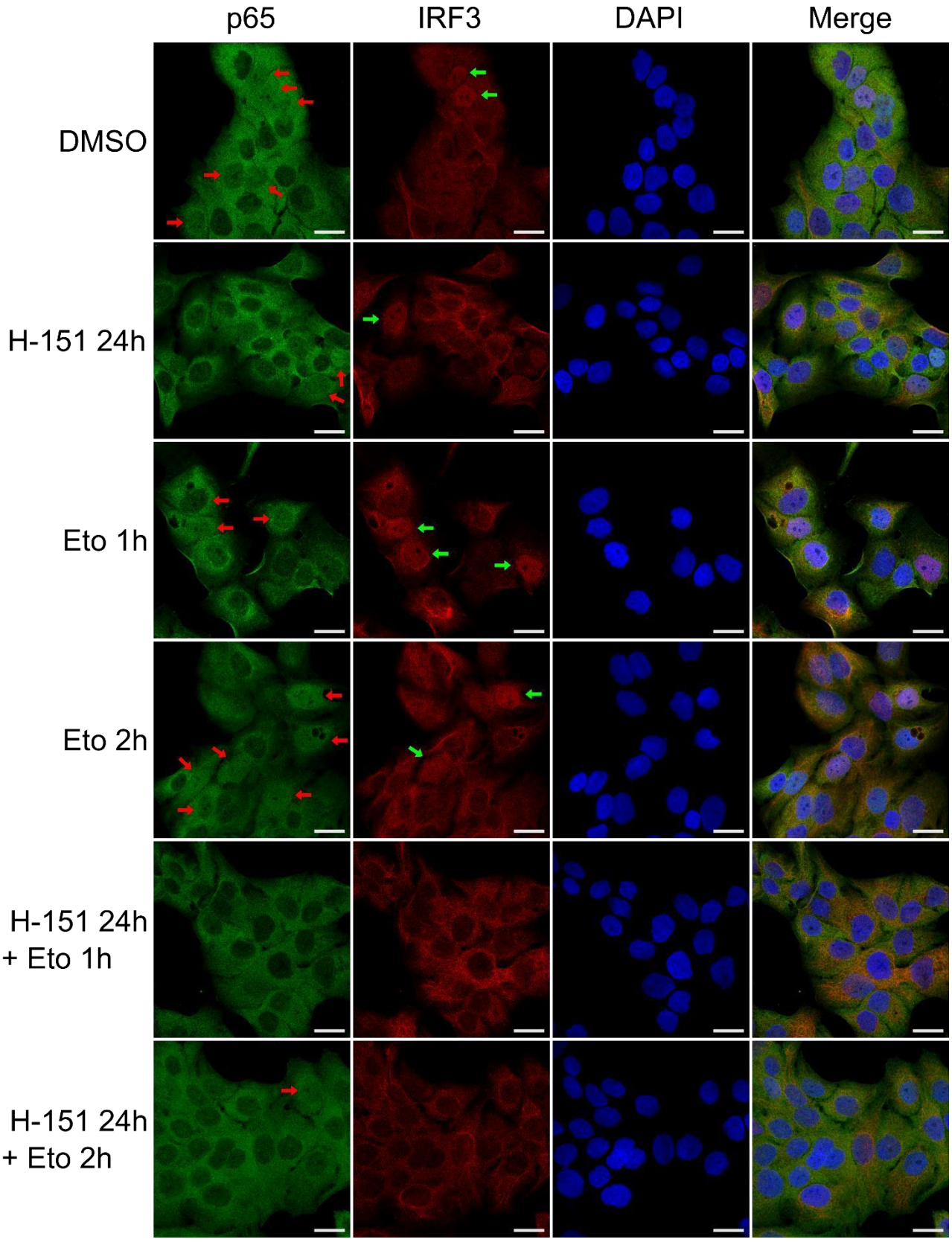

HaCaT STING V155M without doxycycline **(C)**

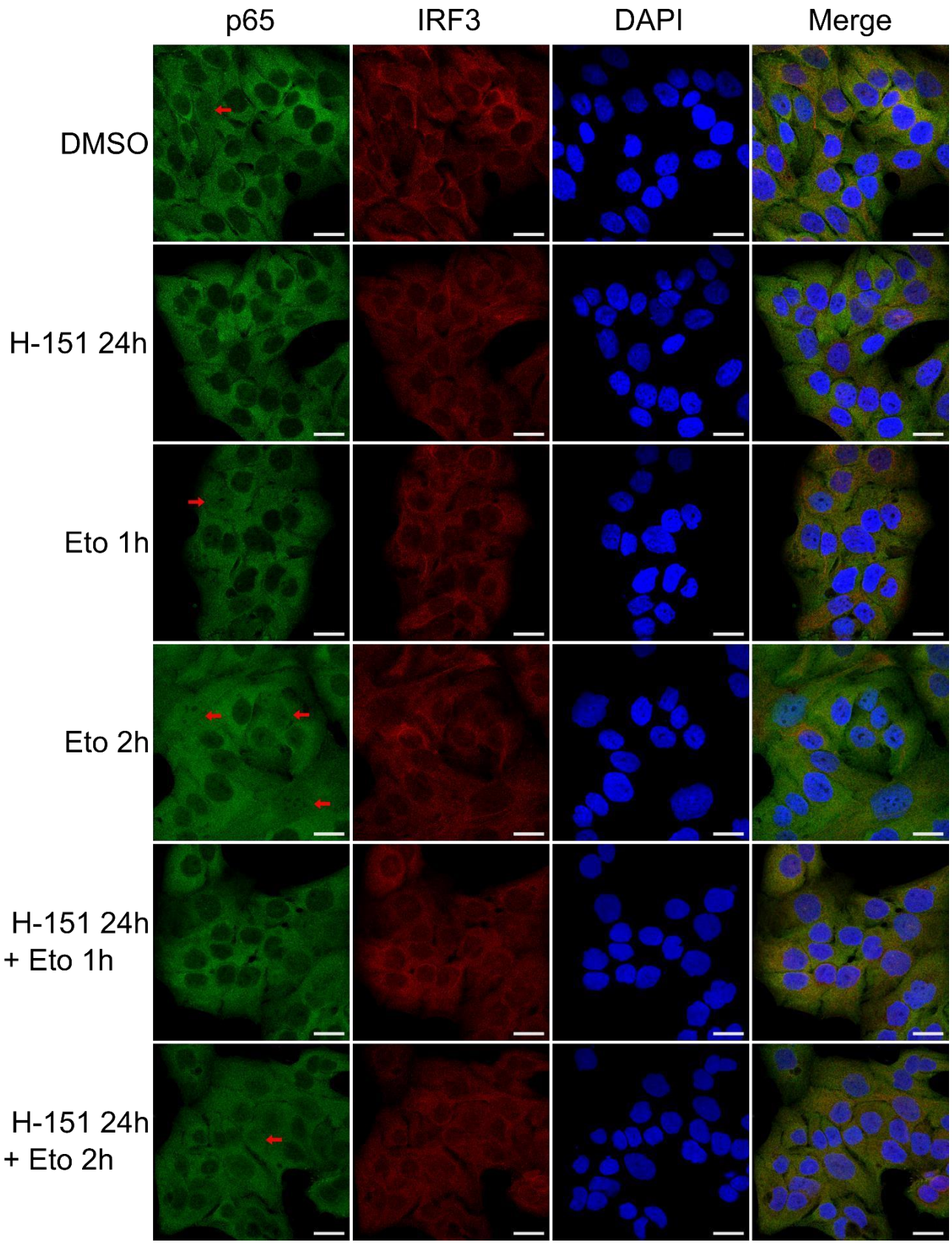

Figure 14. Comparison of p65 and IRF3 nuclear import in WT HaCaT and SAVI cells in response to etoposide and H-151.

*WT HaCaT (**A**) HaCaT STING V155M cells were grown on coverslips and treated with 4μg/mL H-151 for 24h prior to 50μM etoposide or DMSO for 2 hours. SAVI cells were treated with 1μg/ml doxycycline (**B**) for 24h prior to etoposide or DMSO (**C**). Coverslips were stained for DNA (DAPI, blue), NF-κB p65 (green), and IRF3 (red). p65 and IRF-3 nuclear import are indicated by red and green arrows, respectively. Scale bar, 20μm.*

3.3 Elevated inflammatory cytokine expression in STING V155M cells

Quantitative real-time PCR was conducted on DMSO, and etoposide treated WT HaCaT and SAVI doxy cells to evaluate quantitative levels of cytokine mRNA. Interestingly, expression of CCL2 (***Figure 15A***), CCL20 (***Figure 15B***), and IL-6 (***Figure 15C***) was greater in both cell lines in response to etoposide compared to DMSO controls. SAVI doxy cells in general induced a stronger cytokine response to etoposide compared to WT HaCaT cells. Intriguingly, baseline cytokine (CCL2, CCL20, and IL-6) expression from DMSO treated SAVI doxy cells was greater than that of the WT control, indicating constitutive hyperexpression expression in correlation with constitutive p65 phosphorylation in ***Figure 13*** and NF-κB nuclear import in ***Figure 14B***.

Surprisingly, ***Figures 15A-C*** showed somewhat elevated levels of cytokine expression in SAVI cells that were not treated with doxycycline (SAVI no doxy), which should not be expressing STING V155M. Expression of CCL20 and IL-6 in SAVI no doxy cells increased in response to etoposide, even though to a lesser extent than in doxycycline-treated SAVI cells. This correlates with NF-κB nuclear induction in SAVI no doxy cells previously seen in ***Figure 14C***.

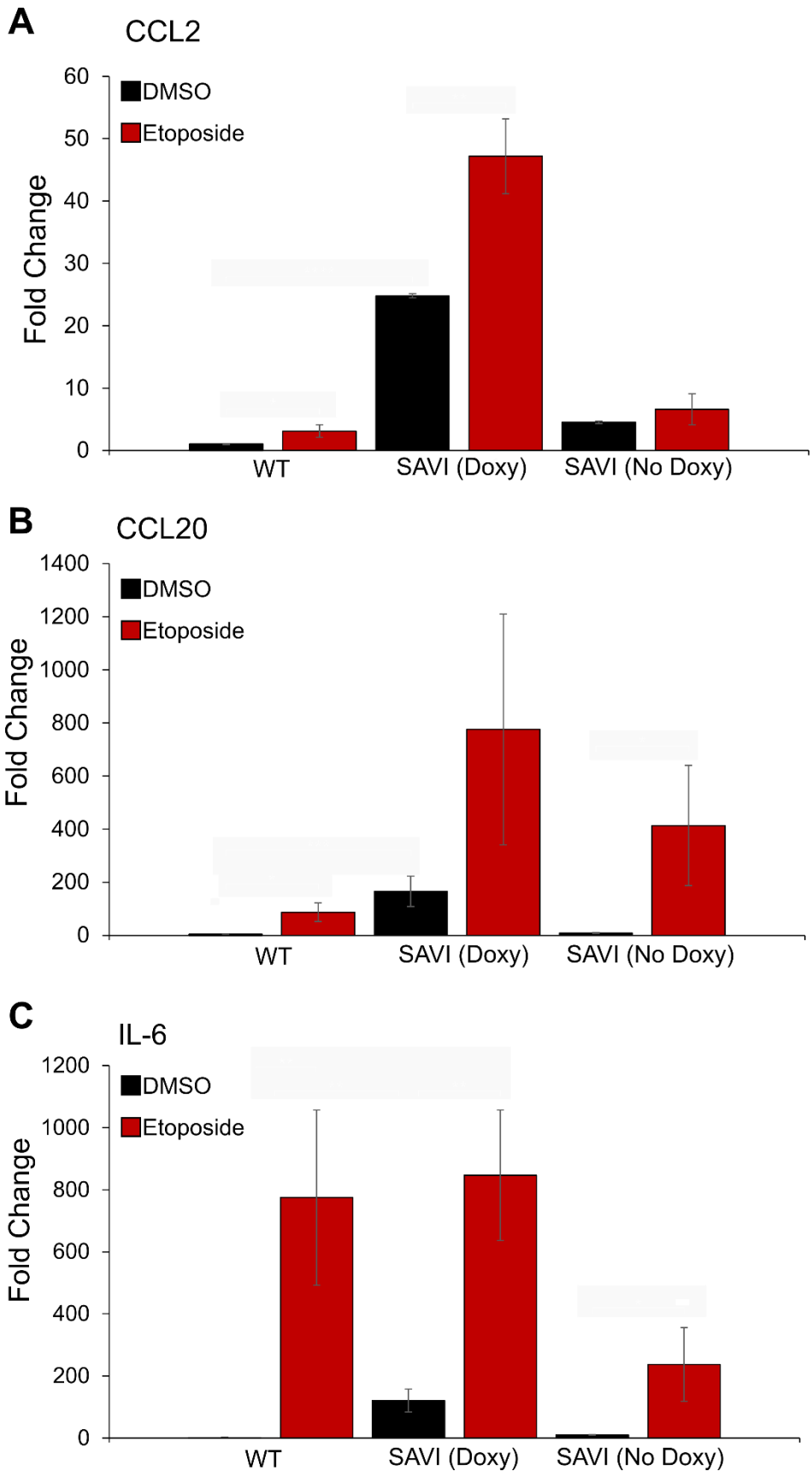

Figure 15. qPCR analysis of etoposide-induced cytokine and chemokine expression in WT HaCaT and STING V155M (SAVI) cells.

HaCaT SAVI (Doxy) were treated with 1µg/ml doxycycline for 24h prior to stimulation. HaCaT cells for were treated with 50µM etoposide or DMSO for 9h. Shown are mean values of technical repeats, error bars represent standard deviations (n = 1).

To quantify levels of CCL20 secretion, ELISA was conducted on WT HaCaT and SAVI cells as seen in ***Figure 16***. Interestingly, basal CCL20 secretion from SAVI cells was higher than WT HaCaT, in correlation with CCL20 seen in ***Figure 15B***. Furthermore, basal levels from SAVI cells appeared to be greater than WT HaCaT levels upon etoposide treatment, indicating constitutive hyperactivation in SAVI cells. As expected, etoposide treatments on both cell lines induced higher levels of CCL20 secretion compared to the DMSO control. When cells were pre-treated with the STING inhibitor H-151 before exposure to etoposide, CCL20 secretion was decreased. This correlated with the decreased levels of NF-κB and IRF3 nuclear induction observed in H-151 treated WT HaCaT and SAVI doxy cells in ***Figure 14A*** and ***Figure 14B***, respectively. This further indicates that responses to etoposide are induced by WT STING and STING V155M.

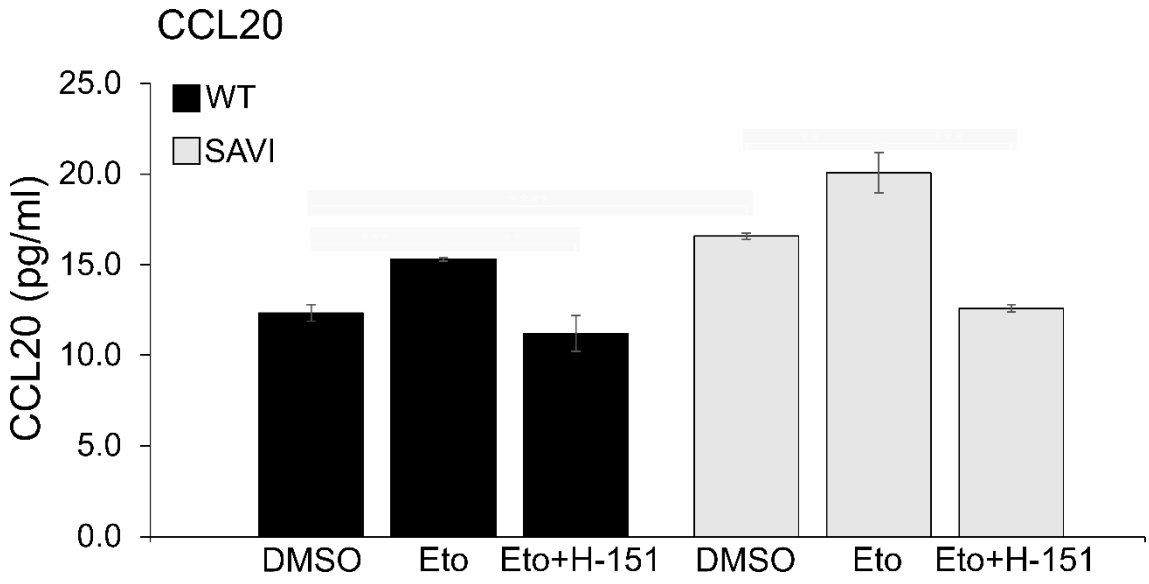

Figure 16. ELISA detection of etoposide-induced CCL20 secretion and suppression by H-151 STING inhibitor from WT HaCaT and STING V155M cells. *HaCaT SAVI cells were treated with 1µg/ml doxycycline for 24h prior to etoposide stimulation. WT HaCaT cells were treated with DMSO for 6h or 4µg/mL*

H-151 for 24h prior to 50μM etoposide treatment for 6h. Shown are mean values of technical repeats, error bars represent standard deviations (n = 1).

To further analyse H-151 inhibition of STING over time, CCL20 secretion was measured in WT HaCaT and doxycycline treated SAVI cells seen in ***Figure 17***. This showed a decrease in baseline WT HaCaT CCL20 secretion after only 3h of H-151 treatment. This was also seen in SAVI doxy cells, but with CCL20 secretion decreased from a higher basal level. Inhibition of CCL20 secretion continued to decrease in both cell lines as H-151 exposure reached 9h. This shows that STING contributes to basal CCL20 secretion in both Wild type and SAVI cells.

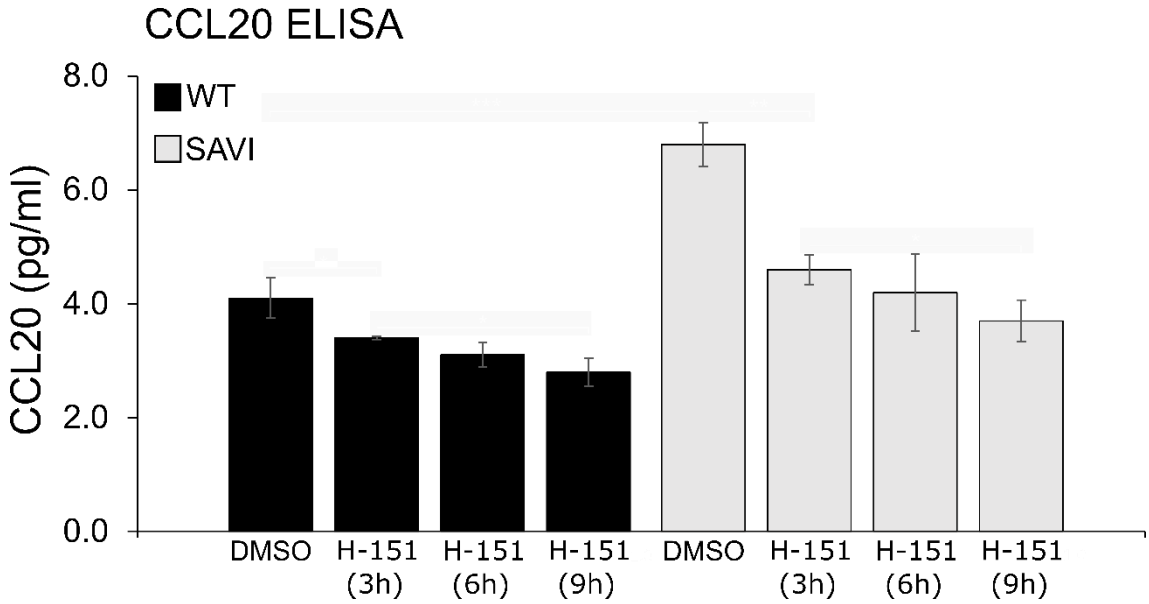

Figure 17. ELISA detection of H-151-induced suppression of CCL20 secretion from WT HaCaT and STING V155M cells.

HaCaT SAVI cells were treated with 1μg/ml doxycycline for 24h prior to H-151 exposure. HaCaT Cells were treated with 4μg/mL H-151 for times indicated or DMSO for 9h. Shown are mean values of technical repeats, error bars represent standard deviations (n = 1).

To address P-p65 bands from ***Figure 13*** and cytokine expression from ***Figure 15*** which showed resemblance between SAVI doxy and SAVI no doxy cells, CCL20 secretion was measured in SAVI no doxy cells treated with etoposide and H-151, as seen in ***Figure 18***. Interestingly, SAVI no doxy cells increased CCL20 secretion in response to etoposide. Furthermore, 24h exposure to the H-151 STING inhibitor decreased baseline and etoposide induced CCL20 secretion.

Overall ***Figure 13***, ***Figure*** 1***4C***, ***Figure*** 1***5A-C***, and ***Figure 18*** shows that there may be some residual SAVI-STING activity in absence of doxycycline treatment.

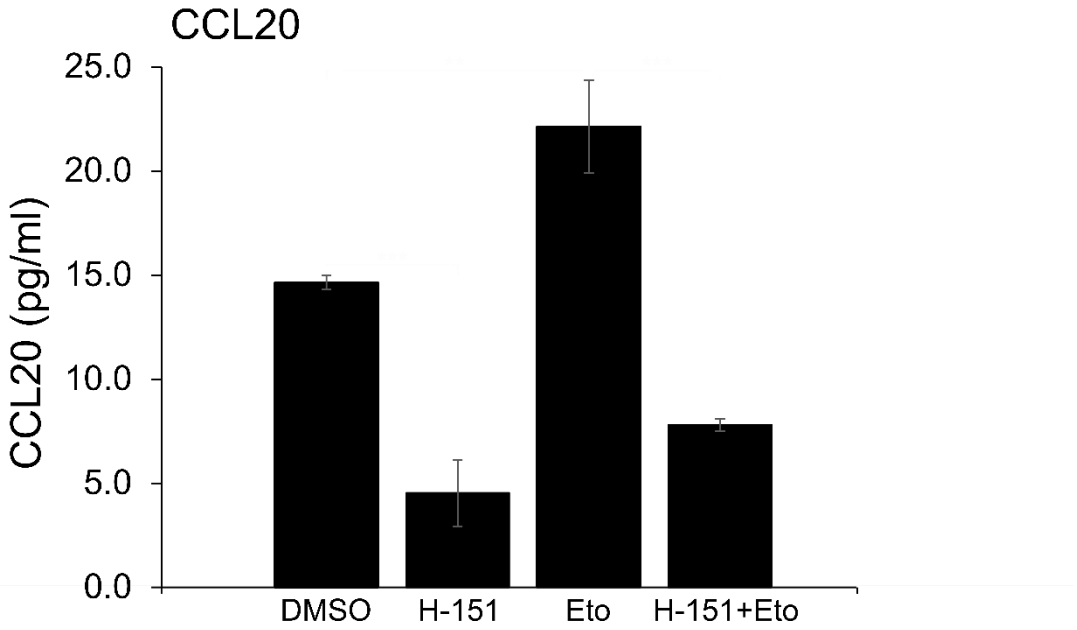

Figure 18. ELISA detection of etoposide-induced CCL20 secretion and suppression by H-151 from HaCaT STING V155M cells without doxycycline induced STING expression.

HaCaT STING V155M cells were treated with DMSO or 50μM etoposide for 6h or 4μg/mL H-151 for 24h prior to etoposide for 6h. Shown are mean values of technical repeats, error bars represent standard deviations (n =1).

4 Discussion

STING associated vasculopathy with onset in infancy is a rare autoinflammatory disorder caused by constitutive STING activation through one of several gain-of function mutations found in the TMEM173 gene (Liu et al., 2014). A case study found that JAK inhibitors used on 17 SAVI patients initially reduced lung and skin inflammation however, only one of the three patients with severe lung inflammation benefited from the IFN inhibitor, with the other two requiring lung transplants (Frémond et al., 2021). The lack of therapeutic efficacy towards the most severe elements of the disease such as fibrotic progression shows further research is needed to find the downstream mechanism activated by the hyperactivating STING mutant. SAVI mouse models showing respiratory failure developing independently of IFN-I in addition to the inconsistency of JAK inhibitors cast doubt upon the pathophysiology relevant to the canonical STINGIRF3-interferon signaling pathway. (Motwani et al., 2019a, Warner et al., 2017). Therefore, it was reasonable to investigate the role of the more recently discovered non-canonical STING-NF-κB pathway that induces a more proinflammatory response that that may be of relevance for the clinical profile of SAVI. Besides SAVI model mice, most studies have utilised HEK293T models with over-expression of STING harbouring SAVI mutations (Melki et al., 2017, Saldanha et al., 2018). HEK293T cells have not demonstrated a functioning noncanonical STING pathway capable of inducing NF-κB induction after DNA damage. To investigate STING V155M hyperactivation this study utilised human HaCaT keratinocytes which have displayed a functioning non-canonical pathway (Dunphy et al., 2018). HaCaT cells are also clinically relevant to SAVI as skin lesions and inflammation that characterise the disease. Therefore, HaCaT cells with STING deleted were stably reconstituted with STING harbouring the V155M mutation under the Tet-On doxycycline-inducible promoter.

The aim of this study was to determine the contribution of the non-canonical STING pathway in the signalling profile of human STING V155M HaCaT cells. We confirmed the expression of HA-tagged STING upon doxycycline treatment by immunoblotting. Confocal microscopy highlighted further contrast between WT and STING V155M. It was clear to observe STING V155M clustering compared to the even distribution of WT STING at the endoplasmic reticulum. Unlike

clustering located at peri-nuclear foci required needed for canonical STING activation, STING V155M clustering was constitutive and not dependent on stimulation with cytosolic DNA (Saitoh et al., 2009, Almine et al., 2017). This was a sign of constitutive activation from the V155M mutant as oligomerisation of STING should only occur after ligand binding resulting in the exposure of the polymerisation interface (Ergun et al., 2019).

Although the proinflammatory signalling profile and phenotype observed from HaCaT SAVI cells could have been induced by hyperactivation of the noncanonical STING pathway, this was not confirmed in this study. Further experiments could have been conducted to confirm this. This would include confirmation that the IRF3 driven canonical STING response was not responsible for the proinflammatory phenotype, in correlation with SAVI mouse models previously discussed. This could have been achieved through treating HaCaT SAVI cells with IRF3 silencing RNA (siRNA) which has previously shown to prevent IRF3 activity in WT Human HaCaT cells (Xu et al., 2014). If the proinflammatory phenotype in the HaCaT SAVI persisted with IRF3 targeted siRNA, inhibition of the non-canonical STING pathway would have been conducted next. Although IFI16 is needed to activate the non-canonical pathway in WT HaCaT cells, its knockout in SAVI cells might not prevent non-canonical activation as SAVI inducing mutations in STING may not require upstream proteins for its activation. BAY 11-7082 (BAY), an inhibitor of IκBα degradation has shown effectiveness in preventing NF-κB in human HaCaT cells in response to DNA damage (Li et al., 2021). Confirming non-canonical hyperactivation through a downstream inhibitor like BAY would justify knocking out individual components of the non-canonical pathway such as IFI-16, TRAF6, and TAK1 to observe proteins that are still required for STING V155M induced hyperactivation of the non-canonical pathway.

Interestingly, Aicardi-Goutières syndrome (AGS), a rare monogenic autoinflammatory disease similar to SAVI and has been observed to be driven by hyperactivation of the canonical STING pathway. AGS patients display elevated levels of IFN-I leading to autoimmunity and a premature death (Rice et al., 2007). The disease is caused by loss-of-function mutations in Trex1, an ER tail anchored

exonuclease that unwinds and degrades cytosolic dsDNA (Yan et al., 2017). The knockout of Trex1 in mice caused hyperactivation of cGAS and overproduction of cGAMP leading to a lethal autoimmune phenotype resembling AGS, which was rescued by the knockout of cGAS (Gao et al., 2015). Trex1 knockout mice exhibited severe inflammation in multiple organs with the heart being most severely affected however, lung inflammation was not reported (Gao et al., 2015). Another ABS mouse model generated through knockout of Trex1 showed autoimmune tissue destruction induced through cGAS, again without lung inflammation reported (Gray et al., 2015). Lastly, mice with a Trex1 loss-offunction mutation (D18N) resulted in an autoinflammatory phenotype with lung inflammation only found surrounding bronchioles, suggesting inhaled antigens contributed to the immune stimulated cells (Grieves et al., 2015). Unlike the SAVI model mice from Bouis et al., 2019, Motwani et al., 2019, and Warner et al., 2017, the AGS model mice did not exhibit chronic lung perivascular inflammation, ulcerative skin lesions, alveolar inflammation and were ameliorated by the knockout of canonical STING pathway components. This difference in pathophysiology between AGS and SAVI mouse models could be due to the activation of different STING pathways.

The resemblance between HaCaT SAVI cells treated with doxycycline or left untreated indicated leaky STING V155M expression, notably after a reduction in CCL20 secretion upon H-151 inhibition. The expression of STING V155M was suspected to be due to activation of the Tet-On system by tetracyclines within the FBS used for HaCaT cell culture. Even low STING V155M expression could increase quickly to detectable levels as release of proinflammatory cytokines from the SAVI inducing mutants have shown to upregulate STING expression via positive feedback (Wang et al., 2021). To prevent leaky expression, Fetal Bovine Serum Tetracycline Negative could have been used instead to culture HaCaT cells. Moreover, the use of a STING knockout instead of untreated HaCaT STING V155M cells would have provided a better control.

A clear trend throughout quantitative analysis of the HaCaT SAVI signalling profile was further hyperactivation in response to etoposide induced DNA damage. This was an interesting finding that implied priming of the non-canonical STING

pathway and capability to be further exacerbated by external stresses in SAVI patients. This could explain high UV sensitivity in SAVI patients resulting in sunburn (Keskitalo et al., 2019). Although STING is often characterised as activating either an IRF3 or NF-kB driven response, STING has been reported to induce other downstream responses. Notably, detection of cytosolic DNA by cGAS in BLaER1 Monocytes has induced cell death through activating potassium efflux upstream of NLRP3, leading to inflammasome activation (Gaidt et al., 2017). Interestingly, STING activation through cGAMP was indispensable for NLRP3 activation however, knockout of TBK1 and the STING S336A mutation that prevents recruitment of IRF3 still permitted inflammasome formation (Gaidt et al., 2017). This is further evidence for STING acting as a signalling hub rather than adaptor protein, which could mean activation of unknown pathways due to SAVI inducing mutations.

The decrease in NF-κB activation and CCL20 expression upon H-151 inhibition demonstrates its potential as a future therapy and an immediate candidate for the use in SAVI mouse models. H-151 has demonstrated safe, selective, and efficacious administration in mouse psoriasis models, suppressing hyperactivated STING and expression of cytokines associated with the noncanonical pathway including IL-1B, TNF-α, and IL-23 (Pan et al., 2021). However, the complete inhibition of STING would compromise the canonical STING pathway and immunity. Deciphering the signalling components required for SAVISTING hyperactivation is critical for development of a pathway specific therapy.

5 Conclusion

The STING adaptor protein has shown to be signalling hub through its cGAS independent non-canonical pathway activation. Induced by DNA damage, this pathway leads to expression of proinflammatory cytokines such as CCL2, CCL20, and IL-6 through NF-kB activation. Our signalling profile analysis of human HaCaT keratinocytes expressing hyperactivated STING V155M found in severe SAVI patients, reveals expression of proinflammatory cytokines at constitutively heightened levels and further induction by DNA damaging agents. This presents valuable information regarding the signalling cascades activated by SAVI-STING and possible insights into a potential novel treatment.

6 References

Ablasser, A., Goldeck, M., Cavlar, T., Deimling, T., Witte, G., Röhl, I., Hopfner, K. P., Ludwig, J. & Hornung, V. (2013). cGAS produces a 2'-5'-linked cyclic dinucleotide second messenger that activates STING. *Nature,* **498:** 380-4.

Agnello, D., Lankford, C. S., Bream, J., Morinobu, A., Gadina, M., O'Shea, J. J. & Frucht, D. M. (2003). Cytokines and transcription factors that regulate T helper cell differentiation: new players and new insights. *J Clin Immunol,* **23:** 147-61.

Ahrens, S., Zelenay, S., Sancho, D., Hanč, P., Kjær, S., Feest, C., Fletcher, G., Durkin, C., Postigo, A., Skehel, M., Batista, F., Thompson, B., Way, M., Reis e Sousa, C. & Schulz, O. (2012). F-actin is an evolutionarily conserved damage-associated molecular pattern recognized by DNGR-1, a receptor for dead cells. *Immunity,* **36:** 635-45.

Akira, S. & Takeda, K. (2004). Toll-like receptor signalling. *Nat Rev Immunol,* **4:** 499-511.

Akira, S., Uematsu, S. & Takeuchi, O. (2006). Pathogen recognition and innate immunity. *Cell,* **124:** 783-801.

Alalwani, S. M., Sierigk, J., Herr, C., Pinkenburg, O., Gallo, R., Vogelmeier, C. & Bals, R. (2010). The antimicrobial peptide LL-37 modulates the inflammatory and host defense response of human neutrophils. *Eur J Immunol,* **40:** 1118-26.

Alexopoulou, L., Holt, A. C., Medzhitov, R. & Flavell, R. A. (2001). Recognition of doublestranded RNA and activation of NF-kappaB by Toll-like receptor 3. *Nature,* **413:** 732-8.

Alghamdi, M. A., Mulla, J., Saheb Sharif-Askari, N., Guzmán-Vega, F. J., Arold, S. T., AbdAlwahed, M., Alharbi, N., Kashour, T. & Halwani, R. (2020). A Novel Biallelic STING1 Gene Variant Causing SAVI in Two Siblings. *Front Immunol,* **11:** 599564.

Almine, J. F., O'Hare, C. A. J., Dunphy, G., Haga, I. R., Naik, R. J., Atrih, A., Connolly, D. J., Taylor, J., Kelsall, I. R., Bowie, A. G., Beard, P. M. & Unterholzner, L. (2017). IFI16 and cGAS cooperate in the activation of STING during DNA sensing in human keratinocytes. *Nature Communications,* **8:** 14392.

Avrameas, S. (2016). Autopolyreactivity Confers a Holistic Role in the Immune System. *Scand J Immunol,* **83:** 227-34.

Azad, A. K., Rajaram, M. V. & Schlesinger, L. S. (2014). Exploitation of the Macrophage Mannose Receptor (CD206) in Infectious Disease Diagnostics and Therapeutics. *J Cytol Mol Biol,* **1**.

Balci, S., Ekinci, R. M. K., de Jesus, A. A., Goldbach-Mansky, R. & Yilmaz, M. (2020). Baricitinib experience on STING-associated vasculopathy with onset in infancy: A representative case from Turkey. *Clin Immunol,* **212:** 108273.

Benatuil, L., Kaye, J., Rich, R. F., Fishman, J. A., Green, W. R. & Iacomini, J. (2005). The influence of natural antibody specificity on antigen immunogenicity. *Eur J Immunol,* **35:** 2638-47.

Benko, S., Philpott, D. J. & Girardin, S. E. (2008). The microbial and danger signals that activate Nod-like receptors. *Cytokine,* **43:** 368-73.

Bernink, J. H., Mjösberg, J. & Spits, H. (2017). Human ILC1: To Be or Not to Be. *Immunity,* **46:** 756-757.

Bertin, J., Nir, W. J., Fischer, C. M., Tayber, O. V., Errada, P. R., Grant, J. R., Keilty, J. J., Gosselin, M. L., Robison, K. E., Wong, G. H., Glucksmann, M. A. & DiStefano, P. S. (1999). Human CARD4 protein is a novel CED-4/Apaf-1 cell death family member that activates NFkappaB. *J Biol Chem,* **274:** 12955-8.

Bettelli, E., Carrier, Y., Gao, W., Korn, T., Strom, T. B., Oukka, M., Weiner, H. L. & Kuchroo, V. K. (2006). Reciprocal developmental pathways for the generation of pathogenic effector TH17 and regulatory T cells. *Nature,* **441:** 235-8.

Beutler, B. (2004). Inferences, questions and possibilities in Toll-like receptor signalling. *Nature,* **430:** 257-63.

Blum, J. S., Wearsch, P. A. & Cresswell, P. (2013). Pathways of antigen processing. *Annu Rev Immunol,* **31:** 443-73.

Borregaard, N. (2010). Neutrophils, from marrow to microbes. *Immunity,* **33:** 657-70.

Boutilier, A. J. & Elsawa, S. F. (2021). Macrophage Polarization States in the Tumor Microenvironment. *Int J Mol Sci,* **22**.

Bowie, A. G. & Unterholzner, L. (2008). Viral evasion and subversion of pattern-recognition receptor signalling. *Nat Rev Immunol,* **8:** 911-22.

Breton, G., Lee, J., Liu, K. & Nussenzweig, M. C. (2015). Defining human dendritic cell progenitors by multiparametric flow cytometry. *Nat Protoc,* **10:** 1407-22.

Brinkmann, V., Reichard, U., Goosmann, C., Fauler, B., Uhlemann, Y., Weiss, D. S., Weinrauch, Y. & Zychlinsky, A. (2004). Neutrophil extracellular traps kill bacteria. *Science,* **303:** 15325.

Brown, G. D., Herre, J., Williams, D. L., Willment, J. A., Marshall, A. S. & Gordon, S. (2003). Dectin-1 mediates the biological effects of beta-glucans. *J Exp Med,* **197:** 1119-24.

Burdette, D. L., Monroe, K. M., Sotelo-Troha, K., Iwig, J. S., Eckert, B., Hyodo, M., Hayakawa, Y. & Vance, R. E. (2011). STING is a direct innate immune sensor of cyclic di-GMP. *Nature,* **478:** 515-8.

Bustamante-Marin, X. M. & Ostrowski, L. E. (2017). Cilia and Mucociliary Clearance. *Cold Spring Harb Perspect Biol,* **9**.

Canitrot, Y., Capp, J. P., Puget, N., Bieth, A., Lopez, B., Hoffmann, J. S. & Cazaux, C. (2004). DNA polymerase beta overexpression stimulates the Rad51-dependent homologous recombination in mammalian cells. *Nucleic Acids Res,* **32:** 5104-12.

Chamaillard, M., Hashimoto, M., Horie, Y., Masumoto, J., Qiu, S., Saab, L., Ogura, Y., Kawasaki, A., Fukase, K., Kusumoto, S., Valvano, M. A., Foster, S. J., Mak, T. W., Nuñez, G. & Inohara, N. (2003). An essential role for NOD1 in host recognition of bacterial peptidoglycan containing diaminopimelic acid. *Nat Immunol,* **4:** 702-7.

Chan, A., Hong, D. L., Atzberger, A., Kollnberger, S., Filer, A. D., Buckley, C. D., McMichael, A., Enver, T. & Bowness, P. (2007). CD56bright human NK cells differentiate into CD56dim cells: role of contact with peripheral fibroblasts. *J Immunol,* **179:** 89-94.

Chariot, A., Leonardi, A., Müller, J., Bonif, M., Brown, K. & Siebenlist, U. (2002). Association of the Adaptor TANK with the IκB Kinase (IKK) Regulator NEMO Connects IKK Complexes with IKKε and TBK1 Kinases. *Journal of Biological Chemistry,* **277:** 37029-37036.

Chen, Y., Park, Y. B., Patel, E. & Silverman, G. J. (2009). IgM antibodies to apoptosis-associated determinants recruit C1q and enhance dendritic cell phagocytosis of apoptotic cells. *J Immunol,* **182:** 6031-43.

Choteau, L., Parny, M., François, N., Bertin, B., Fumery, M., Dubuquoy, L., Takahashi, K., Colombel, J. F., Jouault, T., Poulain, D., Sendid, B. & Jawhara, S. (2016). Role of mannose-binding lectin in intestinal homeostasis and fungal elimination. *Mucosal Immunology,* **9:** 767-776.

Chow, J. C., Young, D. W., Golenbock, D. T., Christ, W. J. & Gusovsky, F. (1999). Toll-like receptor-4 mediates lipopolysaccharide-induced signal transduction. *J Biol Chem,* **274:** 10689-92.

Clarke, S. L. N., Robertson, L., Rice, G. I., Seabra, L., Hilliard, T. N., Crow, Y. J. & Ramanan, A. V. (2020). Type 1 interferonopathy presenting as juvenile idiopathic arthritis with interstitial lung disease: report of a new phenotype. *Pediatr Rheumatol Online J,* **18:** 37. **Cooper, M. D. & Alder, M. N. (**2006). The evolution of adaptive immune systems. *Cell,* **124:** 81522.

Cutolo, M., Campitiello, R., Gotelli, E. & Soldano, S. (2022). The Role of M1/M2 Macrophage Polarization in Rheumatoid Arthritis Synovitis. *Front Immunol,* **13:** 867260.

de Oliveira Mann, C. C., Orzalli, M. H., King, D. S., Kagan, J. C., Lee, A. S. Y. & Kranzusch, P. J. (2019). Modular Architecture of the STING C-Terminal Tail Allows Interferon and NF-κB Signaling Adaptation. *Cell Rep,* **27:** 1165-1175.e5.

de Winther, M. P., Kanters, E., Kraal, G. & Hofker, M. H. (2005). Nuclear factor kappaB signaling in atherogenesis. *Arterioscler Thromb Vasc Biol,* **25:** 904-14.

den Dunnen, J., Gringhuis, S. I. & Geijtenbeek, T. B. (2009). Innate signaling by the C-type lectin DC-SIGN dictates immune responses. *Cancer Immunol Immunother,* **58:** 1149-57.

Deng, X., Xu, M., Yuan, C., Yin, L., Chen, X., Zhou, X., Li, G., Fu, Y., Feghali-Bostwick, C. A. & Pang, L. (2013). Transcriptional regulation of increased CCL2 expression in pulmonary fibrosis involves nuclear factor-κB and activator protein-1. *Int J Biochem Cell Biol,* **45:** 1366-76.

Dobbs, N., Burnaevskiy, N., Chen, D., Gonugunta, V. K., Alto, N. M. & Yan, N. (2015). STING Activation by Translocation from the ER Is Associated with Infection and Autoinflammatory Disease. *Cell Host Microbe,* **18:** 157-68.

Dombrowski, Y., Peric, M., Koglin, S., Kammerbauer, C., Göss, C., Anz, D., Simanski, M., Gläser, R., Harder, J., Hornung, V., Gallo, R. L., Ruzicka, T., Besch, R. & Schauber, J. (2011). Cytosolic DNA triggers inflammasome activation in keratinocytes in psoriatic lesions. *Sci Transl Med,* **3:** 82ra38.

Du Clos, T. W. & Mold, C. (2004). C-Reactive Protein: An Activator of Innate Immunity and a Modulator of Adaptive Immunity. *Immunologic Research,* **30:** 261-278.

Dunphy, G., Flannery, S. M., Almine, J. F., Connolly, D. J., Paulus, C., Jønsson, K. L., Jakobsen, M. R., Nevels, M. M., Bowie, A. G. & Unterholzner, L. (2018). Non-canonical Activation of the DNA Sensing Adaptor STING by ATM and IFI16 Mediates NF-κB Signaling after Nuclear DNA Damage. *Mol Cell,* **71:** 745-760.e5.

Ergun, S. L., Fernandez, D., Weiss, T. M. & Li, L. (2019). STING Polymer Structure Reveals Mechanisms for Activation, Hyperactivation, and Inhibition. *Cell,* **178:** 290-301.e10.

Fauriat, C., Long, E. O., Ljunggren, H. G. & Bryceson, Y. T. (2010). Regulation of human NK-cell cytokine and chemokine production by target cell recognition. *Blood,* **115:** 2167-76.

Feinberg, H., Jégouzo, S. A. F., Rex, M. J., Drickamer, K., Weis, W. I. & Taylor, M. E. (2017). Mechanism of pathogen recognition by human dectin-2. *J Biol Chem,* **292:** 13402-13414. **Fenech, M., Knasmueller, S., Bolognesi, C., Holland, N., Bonassi, S. & Kirsch-Volders, M. (**2020). Micronuclei as biomarkers of DNA damage, aneuploidy, inducers of chromosomal hypermutation and as sources of pro-inflammatory DNA in humans. *Mutat Res Rev Mutat Res,* **786:** 108342.

Ferraboschi, P., Ciceri, S. & Grisenti, P. (2021). Applications of Lysozyme, an Innate Immune Defense Factor, as an Alternative Antibiotic. *Antibiotics (Basel),* **10**.

Fogg, D. K., Sibon, C., Miled, C., Jung, S., Aucouturier, P., Littman, D. R., Cumano, A. & Geissmann, F. (2006). A clonogenic bone marrow progenitor specific for macrophages and dendritic cells. *Science,* **311:** 83-7.

Franchi, L., Eigenbrod, T., Muñoz-Planillo, R. & Nuñez, G. (2009). The inflammasome: a caspase1-activation platform that regulates immune responses and disease pathogenesis. *Nature Immunology,* **10:** 241-247.

Frémond, M. L., Hadchouel, A., Berteloot, L., Melki, I., Bresson, V., Barnabei, L., Jeremiah, N., Belot, A., Bondet, V., Brocq, O., Chan, D., Dagher, R., Dubus, J. C., Duffy, D., FeuilletSoummer, S., Fusaro, M., Gattorno, M., Insalaco, A., Jeziorski, E., Kitabayashi,

N., Lopez-Corbeto, M., Mazingue, F., Morren, M. A., Rice, G. I., Rivière, J. G., Seabra, L., Sirvente, J., Soler-Palacin, P., Stremler-Le Bel, N., Thouvenin, G., Thumerelle, C., Van Aerde, E., Volpi, S., Willcocks, S., Wouters, C., Breton, S., Molina, T., Bader-Meunier, B., Moshous, D., Fischer, A., Blanche, S., Rieux-Laucat, F., Crow, Y. J. & Neven, B. (2021). Overview of STING-Associated Vasculopathy with Onset in Infancy (SAVI) Among 21 Patients. *J Allergy Clin Immunol Pract,* **9:** 803-818.e11.

Frémond, M. L., Rodero, M. P., Jeremiah, N., Belot, A., Jeziorski, E., Duffy, D., Bessis, D., Cros, G., Rice, G. I., Charbit, B., Hulin, A., Khoudour, N., Caballero, C. M., Bodemer, C., Fabre, M., Berteloot, L., Le Bourgeois, M., Reix, P., Walzer, T., Moshous, D., Blanche, S., Fischer, A., Bader-Meunier, B., Rieux-Laucat, F., Crow, Y. J. & Neven, B. (2016). Efficacy of the Janus kinase 1/2 inhibitor ruxolitinib in the treatment of vasculopathy associated with TMEM173-activating mutations in 3 children. *J Allergy Clin Immunol,* **138:** 17521755.

Fu, X., Liu, H., Huang, G. & Dai, S. S. (2021). The emerging role of neutrophils in autoimmuneassociated disorders: effector, predictor, and therapeutic targets. *MedComm,* **2:** 402413.

Funakoshi-Tago, M., Tago, K., Sato, Y., Tominaga, S. & Kasahara, T. (2011). JAK2 is an important signal transducer in IL-33-induced NF-κB activation. *Cell Signal,* **23:** 363-70.

Ganser-Pornillos, B. K. & Pornillos, O. (2019). Restriction of HIV-1 and other retroviruses by TRIM5. *Nat Rev Microbiol,* **17:** 546-556.

Geijtenbeek, T. B. & Gringhuis, S. I. (2009). Signalling through C-type lectin receptors: shaping immune responses. *Nat Rev Immunol,* **9:** 465-79.

Gorjestani, S., Darnay, B. G. & Lin, X. (2012). Tumor necrosis factor receptor-associated factor 6 (TRAF6) and TGFβ-activated kinase 1 (TAK1) play essential roles in the C-type lectin receptor signaling in response to Candida albicans infection. *J Biol Chem,* **287:** 4414350. **Gringhuis, S. I., den Dunnen, J., Litjens, M., van Het Hof, B., van Kooyk, Y. & Geijtenbeek, T. B. (**2007). C-type lectin DC-SIGN modulates Toll-like receptor signaling via Raf-1 kinasedependent acetylation of transcription factor NF-kappaB. *Immunity,* **26:** 605-16.

Gui, X., Yang, H., Li, T., Tan, X., Shi, P., Li, M., Du, F. & Chen, Z. J. (2019). Autophagy induction via STING trafficking is a primordial function of the cGAS pathway. *Nature,* **567:** 262-266.

Guilliams, M., Bruhns, P., Saeys, Y., Hammad, H. & Lambrecht, B. N. (2014). The function of Fcγ receptors in dendritic cells and macrophages. *Nature Reviews Immunology,* **14:** 94-108.

Haag, S. M., Gulen, M. F., Reymond, L., Gibelin, A., Abrami, L., Decout, A., Heymann, M., van der Goot, F. G., Turcatti, G., Behrendt, R. & Ablasser, A. (2018). Targeting STING with covalent small-molecule inhibitors. *Nature,* **559:** 269-273.

Hadjadj, J., Frémond, M. L. & Neven, B. (2021). Emerging Place of JAK Inhibitors in the Treatment of Inborn Errors of Immunity. *Front Immunol,* **12:** 717388.

Haller, O., Staeheli, P., Schwemmle, M. & Kochs, G. (2015). Mx GTPases: dynamin-like antiviral machines of innate immunity. *Trends Microbiol,* **23:** 154-63.

Harton, J. A., Linhoff, M. W., Zhang, J. & Ting, J. P. (2002). Cutting edge: CATERPILLER: a large family of mammalian genes containing CARD, pyrin, nucleotide-binding, and leucine-rich repeat domains. *J Immunol,* **169:** 4088-93.

Hei, L. & Zhong, J. (2017). Laboratory of genetics and physiology 2 (LGP2) plays an essential role in hepatitis C virus infection-induced interferon responses. *Hepatology,* **65:** 1478-1491.

Hernanz-Falcón, P., Joffre, O., Williams, D. L. & Reis e Sousa, C. (2009). Internalization of Dectin1 terminates induction of inflammatory responses. *Eur J Immunol,* **39:** 507-13.

Hinz, M., Stilmann, M., Arslan, S., Khanna, K. K., Dittmar, G. & Scheidereit, C. (2010). A cytoplasmic ATM-TRAF6-cIAP1 module links nuclear DNA damage signaling to ubiquitinmediated NF-κB activation. *Mol Cell,* **40:** 63-74.

Hisamatsu, T., Suzuki, M., Reinecker, H. C., Nadeau, W. J., McCormick, B. A. & Podolsky, D. K. (2003). CARD15/NOD2 functions as an antibacterial factor in human intestinal epithelial cells. *Gastroenterology,* **124:** 993-1000.

Hochrainer, K., Racchumi, G. & Anrather, J. (2013). Site-specific phosphorylation of the p65 protein subunit mediates selective gene expression by differential NF-κB and RNA polymerase II promoter recruitment. *J Biol Chem,* **288:** 285-93.

Hoover, D. L., Berger, M., Nacy, C. A., Hockmeyer, W. T. & Meltzer, M. S. (1984). Killing of Leishmania tropica amastigotes by factors in normal human serum. *J Immunol,* **132:** 893-7.

Hoppstädter, J., Diesel, B., Zarbock, R., Breinig, T., Monz, D., Koch, M., Meyerhans, A., Gortner, L., Lehr, C. M., Huwer, H. & Kiemer, A. K. (2010). Differential cell reaction upon Toll-like receptor 4 and 9 activation in human alveolar and lung interstitial macrophages. *Respir Res,* **11:** 124.

Hornung, V., Ellegast, J., Kim, S., Brzózka, K., Jung, A., Kato, H., Poeck, H., Akira, S., Conzelmann, K. K., Schlee, M., Endres, S. & Hartmann, G. (2006). 5'-Triphosphate RNA is the ligand for RIG-I. *Science,* **314:** 994-7.

Hsu, Y. M., Zhang, Y., You, Y., Wang, D., Li, H., Duramad, O., Qin, X. F., Dong, C. & Lin, X. (2007). The adaptor protein CARD9 is required for innate immune responses to intracellular pathogens. *Nat Immunol,* **8:** 198-205.

Inohara, N., Koseki, T., del Peso, L., Hu, Y., Yee, C., Chen, S., Carrio, R., Merino, J., Liu, D., Ni, J. & Núñez, G. (1999). Nod1, an Apaf-1-like activator of caspase-9 and nuclear factorkappaB. *J Biol Chem,* **274:** 14560-7.

Janeway, C. A., Jr. & Medzhitov, R. (2002). Innate immune recognition. *Annu Rev Immunol,* **20:** 197-216.

Jiang, W., Swiggard, W. J., Heufler, C., Peng, M., Mirza, A., Steinman, R. M. & Nussenzweig, M. C. (1995). The receptor DEC-205 expressed by dendritic cells and thymic epithelial cells is involved in antigen processing. *Nature,* **375:** 151-155.

Jongbloed, S. L., Kassianos, A. J., McDonald, K. J., Clark, G. J., Ju, X., Angel, C. E., Chen, C. J., Dunbar, P. R., Wadley, R. B., Jeet, V., Vulink, A. J., Hart, D. N. & Radford, K. J. (2010). Human CD141+ (BDCA-3)+ dendritic cells (DCs) represent a unique myeloid DC subset that cross-presents necrotic cell antigens. *J Exp Med,* **207:** 1247-60.

Jurisić, V. (2006). [Characteristics of natural killer cell]. *Srp Arh Celok Lek,* **134:** 71-6.

Kahn, S. J., Wleklinski, M., Ezekowitz, R. A., Coder, D., Aruffo, A. & Farr, A. (1996). The major surface glycoprotein of Trypanosoma cruzi amastigotes are ligands of the human serum mannose-binding protein. *Infect Immun,* **64:** 2649-56.

Kalia, N., Singh, J. & Kaur, M. (2021). The ambiguous role of mannose-binding lectin (MBL) in human immunity. *Open Med (Wars),* **16:** 299-310.

Kato, H., Sato, S., Yoneyama, M., Yamamoto, M., Uematsu, S., Matsui, K., Tsujimura, T., Takeda, K., Fujita, T., Takeuchi, O. & Akira, S. (2005). Cell type-specific involvement of RIG-I in antiviral response. *Immunity,* **23:** 19-28.

Kato, H., Takeuchi, O., Mikamo-Satoh, E., Hirai, R., Kawai, T., Matsushita, K., Hiiragi, A., Dermody, T. S., Fujita, T. & Akira, S. (2008). Length-dependent recognition of doublestranded ribonucleic acids by retinoic acid-inducible gene-I and melanoma differentiation-associated gene 5. *J Exp Med,* **205:** 1601-10.

Kato, H., Takeuchi, O., Sato, S., Yoneyama, M., Yamamoto, M., Matsui, K., Uematsu, S., Jung, A., Kawai, T., Ishii, K. J., Yamaguchi, O., Otsu, K., Tsujimura, T., Koh, C. S., Reis e Sousa, C., Matsuura, Y., Fujita, T. & Akira, S. (2006). Differential roles of MDA5 and RIG-I helicases in the recognition of RNA viruses. *Nature,* **441:** 101-5.

Keskitalo, S., Haapaniemi, E., Einarsdottir, E., Rajamäki, K., Heikkilä, H., Ilander, M., Pöyhönen, M., Morgunova, E., Hokynar, K., Lagström, S., Kivirikko, S., Mustjoki, S., Eklund, K., Saarela, J., Kere, J., Seppänen, M. R. J., Ranki, A., Hannula-Jouppi, K. & Varjosalo, M. (2019). Novel TMEM173 Mutation and the Role of Disease Modifying Alleles. *Front Immunol,* **10:** 2770.

Kim, K. D., Zhao, J., Auh, S., Yang, X., Du, P., Tang, H. & Fu, Y. X. (2007). Adaptive immune cells temper initial innate responses. *Nat Med,* **13:** 1248-52.

Kim, S., Poursine-Laurent, J., Truscott, S. M., Lybarger, L., Song, Y. J., Yang, L., French, A. R., Sunwoo, J. B., Lemieux, S., Hansen, T. H. & Yokoyama, W. M. (2005). Licensing of natural killer cells by host major histocompatibility complex class I molecules. *Nature,* **436:** 70913.

Klune, J. R., Dhupar, R., Cardinal, J., Billiar, T. R. & Tsung, A. (2008). HMGB1: endogenous danger signaling. *Mol Med,* **14:** 476-84.

Krabbendam, L., Bernink, J. H. & Spits, H. (2021). Innate lymphoid cells: from helper to killer. *Curr Opin Immunol,* **68:** 28-33.

Land, W., Schneeberger, H., Schleibner, S., Illner, W. D., Abendroth, D., Rutili, G., Arfors, K. E. & Messmer, K. (1994). The beneficial effect of human recombinant superoxide dismutase on acute and chronic rejection events in recipients of cadaveric renal transplants. *Transplantation,* **57:** 211-7.

Lee, W. L., Harrison, R. E. & Grinstein, S. (2003). Phagocytosis by neutrophils. *Microbes Infect,* **5:** 1299-306.

Lemaitre, B., Nicolas, E., Michaut, L., Reichhart, J. M. & Hoffmann, J. A. (1996). The dorsoventral regulatory gene cassette spätzle/Toll/cactus controls the potent antifungal response in Drosophila adults. *Cell,* **86:** 973-83.

Liao, J. C., Lam, R., Brazda, V., Duan, S., Ravichandran, M., Ma, J., Xiao, T., Tempel, W., Zuo, X., Wang, Y. X., Chirgadze, N. Y. & Arrowsmith, C. H. (2011). Interferon-inducible protein 16: insight into the interaction with tumor suppressor p53. *Structure,* **19:** 418-29.

Liao, Y., Goraya, M. U., Yuan, X., Zhang, B., Chiu, S. H. & Chen, J. L. (2019). Functional Involvement of Interferon-Inducible Transmembrane Proteins in Antiviral Immunity. *Front Microbiol,* **10:** 1097.

Lim, A. I., Li, Y., Lopez-Lastra, S., Stadhouders, R., Paul, F., Casrouge, A., Serafini, N., Puel, A., Bustamante, J., Surace, L., Masse-Ranson, G., David, E., Strick-Marchand, H., Le Bourhis, L., Cocchi, R., Topazio, D., Graziano, P., Muscarella, L. A., Rogge, L., Norel, X., Sallenave, J.-M., Allez, M., Graf, T., Hendriks, R. W., Casanova, J.-L., Amit, I., Yssel, H. & Di Santo, J. P. (2017). Systemic Human ILC Precursors Provide a Substrate for Tissue ILC Differentiation. *Cell,* **168:** 1086-1100.e10.

Lim, X., Tan, S. H., Koh, W. L., Chau, R. M., Yan, K. S., Kuo, C. J., van Amerongen, R., Klein, A. M. & Nusse, R. (2013). Interfollicular epidermal stem cells self-renew via autocrine Wnt signaling. *Science,* **342:** 1226-30.

Liu, S., Cai, X., Wu, J., Cong, Q., Chen, X., Li, T., Du, F., Ren, J., Wu, Y. T., Grishin, N. V. & Chen, Z. J. (2015). Phosphorylation of innate immune adaptor proteins MAVS, STING, and TRIF induces IRF3 activation. *Science,* **347:** aaa2630.

Liu, Y., Jesus, A. A., Marrero, B., Yang, D., Ramsey, S. E., Montealegre Sanchez, G. A., Tenbrock, K., Wittkowski, H., Jones, O. Y., Kuehn, H. S., Lee, C.-C. R., Dimattia, M. A., Cowen, E.

W., Gonzalez, B., Palmer, I., Digiovanna, J. J., Biancotto, A., Kim, H., Tsai, W. L., Trier, A. M., Huang, Y., Stone, D. L., Hill, S., Kim, H. J., St. Hilaire, C., Gurprasad, S., Plass, N., Chapelle, D., Horkayne-Szakaly, I., Foell, D., Barysenka, A., Candotti, F., Holland, S. M., Hughes, J. D., Mehmet, H., Issekutz, A. C., Raffeld, M., McElwee, J., Fontana, J. R., Minniti, C. P., Moir, S., Kastner, D. L., Gadina, M., Steven, A. C., Wingfield, P. T., Brooks, S. R., Rosenzweig, S. D., Fleisher, T. A., Deng, Z., Boehm, M., Paller, A. S. & GoldbachMansky, R. (2014). Activated STING in a Vascular and Pulmonary Syndrome. *New England Journal of Medicine,* **371:** 507-518.

Lundberg, K., Rydnert, F., Greiff, L. & Lindstedt, M. (2014). Human blood dendritic cell subsets exhibit discriminative pattern recognition receptor profiles. *Immunology,* **142:** 279-88.

Martinez, F. O. & Gordon, S. (2014). The M1 and M2 paradigm of macrophage activation: time for reassessment. *F1000Prime Rep,* **6:** 13.

Martinsen, J. T., Gunst, J. D., Højen, J. F., Tolstrup, M. & Søgaard, O. S. (2020). The Use of TollLike Receptor Agonists in HIV-1 Cure Strategies. *Front Immunol,* **11:** 1112.

Martínez-Lostao, L., Anel, A. & Pardo, J. (2015). How Do Cytotoxic Lymphocytes Kill Cancer Cells? *Clin Cancer Res,* **21:** 5047-56.

Matzinger, P. (1994). Tolerance, danger, and the extended family. *Annu Rev Immunol,* **12:** 9911045.

Mayadas, T. N., Cullere, X. & Lowell, C. A. (2014). The multifaceted functions of neutrophils. *Annu Rev Pathol,* **9:** 181-218.

McNab, F., Mayer-Barber, K., Sher, A., Wack, A. & O'Garra, A. (2015). Type I interferons in infectious disease. *Nat Rev Immunol,* **15:** 87-103.

Merle, N. S., Church, S. E., Fremeaux-Bacchi, V. & Roumenina, L. T. (2015). Complement System Part I - Molecular Mechanisms of Activation and Regulation. *Front Immunol,* **6:** 262.

Mold, C., Baca, R. & Du Clos, T. W. (2002). Serum amyloid P component and C-reactive protein opsonize apoptotic cells for phagocytosis through Fcgamma receptors. *J Autoimmun,* **19:** 147-54.

Mold, C., Gresham, H. D. & Du Clos, T. W. (2001). Serum amyloid P component and C-reactive protein mediate phagocytosis through murine Fc gamma Rs. *J Immunol,* **166:** 1200-5.

Motwani, M., Pawaria, S., Bernier, J., Moses, S., Henry, K., Fang, T., Burkly, L., MarshakRothstein, A. & Fitzgerald, K. A. (2019a). Hierarchy of clinical manifestations in SAVI N153S and V154M mouse models. *Proc Natl Acad Sci U S A,* **116:** 7941-7950.

Motwani, M., Pesiridis, S. & Fitzgerald, K. A. (2019b). DNA sensing by the cGAS–STING pathway in health and disease. *Nature Reviews Genetics,* **20:** 657-674.

Mukai, K., Konno, H., Akiba, T., Uemura, T., Waguri, S., Kobayashi, T., Barber, G. N., Arai, H. & Taguchi, T. (2016). Activation of STING requires palmitoylation at the Golgi. *Nat Commun,* **7:** 11932.

Neth, O., Jack, D. L., Dodds, A. W., Holzel, H., Klein, N. J. & Turner, M. W. (2000). Mannosebinding lectin binds to a range of clinically relevant microorganisms and promotes complement deposition. *Infect Immun,* **68:** 688-93.

Ni, X., Ru, H., Ma, F., Zhao, L., Shaw, N., Feng, Y., Ding, W., Gong, W., Wang, Q., Ouyang, S., Cheng, G. & Liu, Z. J. (2016). New insights into the structural basis of DNA recognition by HINa and HINb domains of IFI16. *J Mol Cell Biol,* **8:** 51-61.

Niyonsaba, F., Kiatsurayanon, C., Chieosilapatham, P. & Ogawa, H. (2017). Friends or Foes? Host defense (antimicrobial) peptides and proteins in human skin diseases. *Exp Dermatol,* **26:** 989-998.

Niyonsaba, F., Someya, A., Hirata, M., Ogawa, H. & Nagaoka, I. (2001). Evaluation of the effects of peptide antibiotics human beta-defensins-1/-2 and LL-37 on histamine release and prostaglandin D(2) production from mast cells. *Eur J Immunol,* **31:** 1066-75.

O'Neill, L. A. J. & Bowie, A. G. (2007). The family of five: TIR-domain-containing adaptors in Tolllike receptor signalling. *Nature Reviews Immunology,* **7:** 353-364.

Oganesyan, G., Saha, S. K., Guo, B., He, J. Q., Shahangian, A., Zarnegar, B., Perry, A. & Cheng, G. (2006). Critical role of TRAF3 in the Toll-like receptor-dependent and -independent antiviral response. *Nature,* **439:** 208-11.

Ogura, Y., Inohara, N., Benito, A., Chen, F. F., Yamaoka, S. & Nunez, G. (2001). Nod2, a Nod1/Apaf-1 family member that is restricted to monocytes and activates NF-kappaB. *J Biol Chem,* **276:** 4812-8.

Ojcius, D. & Saïd-Sadier, N. (2012). Alarmins, inflammasomes and immunity. *Biomedical Journal,* **35:** 437.

Othman, A., Sekheri, M. & Filep, J. G. (2021). Roles of neutrophil granule proteins in orchestrating inflammation and immunity. *The FEBS Journal*.

Pai, S. & Thomas, R. (2008). Immune deficiency or hyperactivity-Nf-kappab illuminates autoimmunity. *J Autoimmun,* **31:** 245-51.

Pan, Y., You, Y., Sun, L., Sui, Q., Liu, L., Yuan, H., Chen, C., Liu, J., Wen, X., Dai, L. & Sun, H. (2021). The STING antagonist H-151 ameliorates psoriasis via suppression of STING/NFκBmediated inflammation. *Br J Pharmacol,* **178:** 4907-4922.

Panda, S. & Ding, J. L. (2015). Natural antibodies bridge innate and adaptive immunity. *J Immunol,* **194:** 13-20.

Perry, A. K., Chow, E. K., Goodnough, J. B., Yeh, W. C. & Cheng, G. (2004). Differential requirement for TANK-binding kinase-1 in type I interferon responses to toll-like receptor activation and viral infection. *J Exp Med,* **199:** 1651-8.

Platanias, L. C. (2005). Mechanisms of type-I- and type-II-interferon-mediated signalling. *Nature Reviews Immunology,* **5:** 375-386.

Prabakaran, T., Troldborg, A., Kumpunya, S., Alee, I., Marinković, E., Windross, S. J., Nandakumar, R., Narita, R., Zhang, B. C., Carstensen, M., Vejvisithsakul, P., Marqvorsen, M. H. S., Iversen, M. B., Holm, C. K., Østergaard, L. J., Pedersen, F. S., Pisitkun, T., Behrendt, R., Pisitkun, P. & Paludan, S. R. (2021). A STING antagonist modulating the interaction with STIM1 blocks ER-to-Golgi trafficking and inhibits lupus pathology. *EBioMedicine,* **66:** 103314.

Pütsep, K., Carlsson, G., Boman, H. G. & Andersson, M. (2002). Deficiency of antibacterial peptides in patients with morbus Kostmann: an observation study. *Lancet,* **360:** 1144-9.

Rawlings, A. V. & Matts, P. J. (2005). Stratum Corneum Moisturization at the Molecular Level: An Update in Relation to the Dry Skin Cycle. *Journal of Investigative Dermatology,* **124:** 1099-1110.

Rehwinkel, J. & Gack, M. U. (2020). RIG-I-like receptors: their regulation and roles in RNA sensing. *Nature Reviews Immunology,* **20:** 537-551.

Reyneveld, G. I., Savelkoul, H. F. J. & Parmentier, H. K. (2020). Current Understanding of Natural Antibodies and Exploring the Possibilities of Modulation Using Veterinary Models. A Review. *Front Immunol,* **11:** 2139.

Rosales, C. (2018). Neutrophil: A Cell with Many Roles in Inflammation or Several Cell Types? *Front Physiol,* **9:** 113.

Saifuddin, M., Hart, M. L., Gewurz, H., Zhang, Y. & Spear, G. T. (2000). Interaction of mannosebinding lectin with primary isolates of human immunodeficiency virus type 1. *J Gen Virol,* **81:** 949-55.

Saito, T., Hirai, R., Loo, Y. M., Owen, D., Johnson, C. L., Sinha, S. C., Akira, S., Fujita, T. & Gale, M., Jr. (2007). Regulation of innate antiviral defenses through a shared repressor domain in RIG-I and LGP2. *Proc Natl Acad Sci U S A,* **104:** 582-7.

Saitoh, T., Fujita, N., Hayashi, T., Takahara, K., Satoh, T., Lee, H., Matsunaga, K., Kageyama, S., Omori, H., Noda, T., Yamamoto, N., Kawai, T., Ishii, K., Takeuchi, O., Yoshimori, T. & Akira, S. (2009). Atg9a controls dsDNA-driven dynamic translocation of STING and the innate immune response. *Proc Natl Acad Sci U S A,* **106:** 20842-6.

Saldanha, R. G., Balka, K. R., Davidson, S., Wainstein, B. K., Wong, M., Macintosh, R., Loo, C. K. C., Weber, M. A., Kamath, V., Moghaddas, F., De Nardo, D., Gray, P. E. & Masters, S. L. (2018). A Mutation Outside the Dimerization Domain Causing Atypical STINGAssociated Vasculopathy With Onset in Infancy. *Front Immunol,* **9:** 1535.

Sameer, A. S. & Nissar, S. (2021). Toll-Like Receptors (TLRs): Structure, Functions, Signaling, and Role of Their Polymorphisms in Colorectal Cancer Susceptibility. *Biomed Res Int,* **2021:** 1157023.

Sancho, D. & Reis e Sousa, C. (2012). Signaling by myeloid C-type lectin receptors in immunity and homeostasis. *Annu Rev Immunol,* **30:** 491-529.

Sandilands, A., Sutherland, C., Irvine, A. D. & McLean, W. H. (2009). Filaggrin in the frontline: role in skin barrier function and disease. *J Cell Sci,* **122:** 1285-94.

Santini, S. M., Lapenta, C., Logozzi, M., Parlato, S., Spada, M., Di Pucchio, T. & Belardelli, F. (2000). Type I interferon as a powerful adjuvant for monocyte-derived dendritic cell development and activity in vitro and in Hu-PBL-SCID mice. *J Exp Med,* **191:** 1777-88.

Savage, H. P. & Baumgarth, N. (2015). Characteristics of natural antibody-secreting cells. *Ann N Y Acad Sci,* **1362:** 132-42.

Scaffidi, P., Misteli, T. & Bianchi, M. E. (2002). Release of chromatin protein HMGB1 by necrotic cells triggers inflammation. *Nature,* **418:** 191-5.

Schlaepfer, E., Rochat, M. A., Duo, L. & Speck, R. F. (2014). Triggering TLR2, -3, -4, -5, and -8 reinforces the restrictive nature of M1- and M2-polarized macrophages to HIV. *J Virol,* **88:** 9769-81.

Schneider, W. M., Chevillotte, M. D. & Rice, C. M. (2014). Interferon-stimulated genes: a complex web of host defenses. *Annu Rev Immunol,* **32:** 513-45.

Serafini, N., Vosshenrich, C. A. & Di Santo, J. P. (2015). Transcriptional regulation of innate lymphoid cell fate. *Nat Rev Immunol,* **15:** 415-28.

Serbina, N. V., Jia, T., Hohl, T. M. & Pamer, E. G. (2008). Monocyte-mediated defense against microbial pathogens. *Annu Rev Immunol,* **26:** 421-52.

Shang, G., Zhang, C., Chen, Z. J., Bai, X. C. & Zhang, X. (2019). Cryo-EM structures of STING reveal its mechanism of activation by cyclic GMP-AMP. *Nature,* **567:** 389-393.

Sica, A. & Mantovani, A. (2012). Macrophage plasticity and polarization: in vivo veritas. *J Clin Invest,* **122:** 787-95.

Siqueira Mietto, B., Kroner, A., Girolami, E. I., Santos-Nogueira, E., Zhang, J. & David, S. (2015). Role of IL-10 in Resolution of Inflammation and Functional Recovery after Peripheral Nerve Injury. *J Neurosci,* **35:** 16431-42.

Sun, L., Wu, J., Du, F., Chen, X. & Chen, Z. J. (2013). Cyclic GMP-AMP synthase is a cytosolic DNA sensor that activates the type I interferon pathway. *Science,* **339:** 786-91.

Sundararaman, S. K. & Barbie, D. A. (2018). Tumor cGAMP Awakens the Natural Killers. *Immunity,* **49:** 585-587.

Tada, H., Aiba, S., Shibata, K., Ohteki, T. & Takada, H. (2005). Synergistic effect of Nod1 and Nod2 agonists with toll-like receptor agonists on human dendritic cells to generate interleukin12 and T helper type 1 cells. *Infect Immun,* **73:** 7967-76.

Takahasi, K., Yoneyama, M., Nishihori, T., Hirai, R., Kumeta, H., Narita, R., Gale, M., Jr., Inagaki, F. & Fujita, T. (2008). Nonself RNA-sensing mechanism of RIG-I helicase and activation of antiviral immune responses. *Mol Cell,* **29:** 428-40.

Thomas, P. G., Dash, P., Aldridge, J. R., Jr., Ellebedy, A. H., Reynolds, C., Funk, A. J., Martin, W. J., Lamkanfi, M., Webby, R. J., Boyd, K. L., Doherty, P. C. & Kanneganti, T. D. (2009). The intracellular sensor NLRP3 mediates key innate and healing responses to influenza A virus via the regulation of caspase-1. *Immunity,* **30:** 566-75.

Ting, J. P., Lovering, R. C., Alnemri, E. S., Bertin, J., Boss, J. M., Davis, B. K., Flavell, R. A., Girardin, S. E., Godzik, A., Harton, J. A., Hoffman, H. M., Hugot, J. P., Inohara, N., Mackenzie, A., Maltais, L. J., Nunez, G., Ogura, Y., Otten, L. A., Philpott, D., Reed, J. C., Reith, W., Schreiber, S., Steimle, V. & Ward, P. A. (2008). The NLR gene family: a standard nomenclature. *Immunity,* **28:** 285-7.

Townsend, R., Read, R. C., Turner, M. W., Klein, N. J. & Jack, D. L. (2001). Differential recognition of obligate anaerobic bacteria by human mannose-binding lectin. *Clin Exp Immunol,* **124:** 223-8.

Viatour, P., Merville, M.-P., Bours, V. & Chariot, A. (2005). Phosphorylation of NF-κB and IκB proteins: implications in cancer and inflammation. *Trends in Biochemical Sciences,* **30:** 43-52.

Viganò, E., Diamond, C. E., Spreafico, R., Balachander, A., Sobota, R. M. & Mortellaro, A. (2015). Human caspase-4 and caspase-5 regulate the one-step non-canonical inflammasome activation in monocytes. *Nature Communications,* **6:** 8761.

Volcic, M., Karl, S., Baumann, B., Salles, D., Daniel, P., Fulda, S. & Wiesmüller, L. (2012). NF-κB regulates DNA double-strand break repair in conjunction with BRCA1-CtIP complexes. *Nucleic Acids Res,* **40:** 181-95.

Voss, E., Wehkamp, J., Wehkamp, K., Stange, E. F., Schröder, J. M. & Harder, J. (2006). NOD2/CARD15 mediates induction of the antimicrobial peptide human beta-defensin2. *J Biol Chem,* **281:** 2005-11.

Walsh, M. C., Lee, J. & Choi, Y. (2015). Tumor necrosis factor receptor- associated factor 6 (TRAF6) regulation of development, function, and homeostasis of the immune system. *Immunol Rev,* **266:** 72-92.

Walzer, T., Dalod, M., Robbins, S. H., Zitvogel, L. & Vivier, E. (2005). Natural-killer cells and dendritic cells: "l'union fait la force". *Blood,* **106:** 2252-8.

Wang, C., Deng, L., Hong, M., Akkaraju, G. R., Inoue, J. & Chen, Z. J. (2001). TAK1 is a ubiquitindependent kinase of MKK and IKK. *Nature,* **412:** 346-51.

Wang, N., Liang, H. & Zen, K. (2014). Molecular mechanisms that influence the macrophage m1m2 polarization balance. *Front Immunol,* **5:** 614.

Wang, S., Zhang, J., Sui, L., Xu, H., Piao, Q., Liu, Y., Qu, X., Sun, Y., Song, L., Li, D., Peng, L., Hua, S., Hu, G. & Chen, J. (2017). Antibiotics induce polarization of pleural macrophages to M2-like phenotype in patients with tuberculous pleuritis. *Scientific Reports,* **7**.

Wang, Y., Wang, F. & Zhang, X. (2021). STING-associated vasculopathy with onset in infancy: a familial case series report and literature review. *Annals of Translational Medicine,* **9:** 176176.

Wang, Z., Wang, X., Zou, H., Dai, Z., Feng, S., Zhang, M., Xiao, G., Liu, Z. & Cheng, Q. (2020). The Basic Characteristics of the Pentraxin Family and Their Functions in Tumor Progression. *Front Immunol,* **11:** 1757.

Warner, J. D., Irizarry-Caro, R. A., Bennion, B. G., Ai, T. L., Smith, A. M., Miner, C. A., Sakai, T., Gonugunta, V. K., Wu, J., Platt, D. J., Yan, N. & Miner, J. J. (2017). STING-associated vasculopathy develops independently of IRF3 in mice. *J Exp Med,* **214:** 3279-3292.

Watanabe, T., Asano, N., Fichtner-Feigl, S., Gorelick, P. L., Tsuji, Y., Matsumoto, Y., Chiba, T., Fuss, I. J., Kitani, A. & Strober, W. (2010). NOD1 contributes to mouse host defense against Helicobacter pylori via induction of type I IFN and activation of the ISGF3 signaling pathway. *J Clin Invest,* **120:** 1645-62.

Wijesundera, K. K., Izawa, T., Murakami, H., Tennakoon, A. H., Golbar, H. M., Kato-Ichikawa, C., Tanaka, M., Kuwamura, M. & Yamate, J. (2014). M1- and M2-macrophage polarization in thioacetamide (TAA)-induced rat liver lesions; a possible analysis for hepatopathology. *Histol Histopathol,* **29:** 497-511.

Wu, K., Jiang, S. W., Thangaraju, M., Wu, G. & Couch, F. J. (2000). Induction of the BRCA2 promoter by nuclear factor-kappa B. *J Biol Chem,* **275:** 35548-56.

Xia, Z. P., Sun, L., Chen, X., Pineda, G., Jiang, X., Adhikari, A., Zeng, W. & Chen, Z. J. (2009). Direct activation of protein kinases by unanchored polyubiquitin chains. *Nature,* **461:** 114-9.

Yamaguchi, Y., Nagase, T., Makita, R., Fukuhara, S., Tomita, T., Tominaga, T., Kurihara, H. & Ouchi, Y. (2002). Identification of multiple novel epididymis-specific beta-defensin isoforms in humans and mice. *J Immunol,* **169:** 2516-23.

Yan, N. & Chen, Z. J. (2012). Intrinsic antiviral immunity. *Nat Immunol,* **13:** 214-22.

Yoneyama, M., Kikuchi, M., Natsukawa, T., Shinobu, N., Imaizumi, T., Miyagishi, M., Taira, K., Akira, S. & Fujita, T. (2004). The RNA helicase RIG-I has an essential function in doublestranded RNA-induced innate antiviral responses. *Nat Immunol,* **5:** 730-7.

Yunna, C., Mengru, H., Lei, W. & Weidong, C. (2020). Macrophage M1/M2 polarization. *Eur J Pharmacol,* **877:** 173090.

Zhang, C., Shang, G., Gui, X., Zhang, X., Bai, X. C. & Chen, Z. J. (2019). Structural basis of STING binding with and phosphorylation by TBK1. *Nature,* **567:** 394-398.

Zhang, J. G., Czabotar, P. E., Policheni, A. N., Caminschi, I., Wan, S. S., Kitsoulis, S., Tullett, K. M., Robin, A. Y., Brammananth, R., van Delft, M. F., Lu, J., O'Reilly, L. A., Josefsson, E. C., Kile, B. T., Chin, W. J., Mintern, J. D., Olshina, M. A., Wong, W., Baum, J., Wright, M. D., Huang, D. C., Mohandas, N., Coppel, R. L., Colman, P. M., Nicola, N. A., Shortman, K. & Lahoud, M. H. (2012). The dendritic cell receptor Clec9A binds damaged cells via exposed actin filaments. *Immunity,* **36:** 646-57.

Zhang, X., Wu, J., Du, F., Xu, H., Sun, L., Chen, Z., Brautigam, C. A. & Chen, Z. J. (2014). The cytosolic DNA sensor cGAS forms an oligomeric complex with DNA and undergoes switch-like conformational changes in the activation loop. *Cell Rep,* **6:** 421-30.

Zhou, W., Whiteley, A. T., de Oliveira Mann, C. C., Morehouse, B. R., Nowak, R. P., Fischer, E. S., Gray, N. S., Mekalanos, J. J. & Kranzusch, P. J. (2018). Structure of the Human cGASDNA Complex Reveals Enhanced Control of Immune Surveillance. *Cell,* **174:** 300311.e11.

Zhou, Z. H., Wild, T., Xiong, Y., Sylvers, L. H., Zhang, Y., Zhang, L., Wahl, L., Wahl, S. M., Kozlowski, S. & Notkins, A. L. (2013). Polyreactive antibodies plus complement enhance the phagocytosis of cells made apoptotic by UV-light or HIV. *Sci Rep,* **3:** 2271.